JOURNAL OF GUIDANCE, CONTROL, AND DYNAMICS
Vol. 32, No. 3, May–June 2009

# Simple Method to Determine Globally Optimal Orbital Transfers

Mauro Pontani*
*University of Rome "La Sapienza," 00184 Rome, Italy*

DOI: 10.2514/1.38143

**This research is intended to describe a simple analytical approach to determine the globally optimal impulsive transfer between two arbitrary Keplerian trajectories, including the case of initial and final elliptic orbits. First, Hohmann and bielliptic transfers are proved to be two possible global optimal transfers between two elliptic orbits without any restriction on the number of impulses. This result is achieved by using ordinary calculus in conjunction with a simple graphical construction. The final choice between these two transfers depends on the apoapse and periapse radii of the initial and final ellipses. In this paper, a simple analytical procedure is proposed that is capable of determining the optimal choice between a Hohmann and bielliptic transfer for arbitrary initial and final orbits. An approach similar to that used for elliptic orbits leads to results of a global nature for transfers that involve both elliptic orbits and escape trajectories.**

## Nomenclature

| | | |
|---|---|---|
| $a$ | = | semimajor axis |
| $E$ | = | trajectory (specific) energy |
| $E_B$ | = | specific energy associated with the generic point B |
| $E_0$ | = | specified value for the specific energy $E$ |
| $e$ | = | eccentricity |
| $f$ | = | true anomaly |
| $\mathbf{h}$ | = | specific angular momentum |
| $h$ | = | magnitude of the specific angular momentum |
| $\mathbf{r}$ | = | position vector |
| $r$ | = | radius |
| $r_A$ | = | apoapse radius (for elliptic orbits only) |
| $r_{AB}$ | = | apoapse radius associated with the generic point B |
| $r_A^{(\max)}$ | = | maximum (allowed) apoapse radius |
| $r_P$ | = | periapse radius |
| $r_{PB}$ | = | periapse radius associated with the generic point B |
| $r_P^{(\min)}$ | = | minimum (allowed) periapse radius |
| $\mathbf{v}$ | = | velocity vector |
| $v$ | = | velocity magnitude |
| $\Delta v_{rP}$ | = | impulse magnitude at apoapse |
| $\Delta v_{P_1 \cdots P_n}$ | = | total velocity change associated with path $P_1 \cdots P_n$ |
| $\Delta v_X$ | = | impulse magnitude at periapse |
| $\mu$ | = | gravitational parameter |

## I. Introduction

THE impulsive-thrust approximation has application in the case of high-thrust rockets and spacecraft and represents a very good approximation [1,2] of the finite-thrust maneuvers that a vehicle performs once it is in orbit, under the assumption that gravitational losses during propulsion can be neglected. In this context, more than 80 years ago, Hohmann [3] conjectured that in an inverse square gravitational field, the minimum fuel transfer between coplanar circular orbits is the bitangent elliptic transfer performed through two tangential impulsive changes of velocity, which occur at the apse points of the transfer orbit. Such a transfer was termed the *Hohmann transfer*, and for a relatively long time, it was assumed to be globally optimal in terms of total velocity change. However, in the late 1950s and early 1960s, Hoelker and Silber [4], Shternfeld [5], and Edelbaum [6] independently proposed the three-impulse bielliptic transfer, which was shown to be more economical than the Hohmann transfer when the initial orbit and the final orbit are sufficiently far apart from each other, and so a midcourse impulse can occur sufficiently far outside the outer orbit. Later, Ting [7] proved the local optimality of the Hohmann transfer and stated that the optimal orientation of the axes of the initial and final (elliptical) orbits is always coaxial and aligned (i.e., with periapses on the same side). In addition, Ting [7] demonstrated that for any orbital transfer at the intersection of two noncoplanar orbits, there exists a corresponding coplanar transfer with lower cost. This circumstance implies that if an orbit is specified only by its specific energy and angular momentum, the minimum cost transfer is unequivocally coplanar (i.e., corresponds to initial, final, and transfer orbits all belonging to the same plane). Finally, Ting [8] also proved that orbital transfers performed through four or more impulses are never optimal.

Proofs of the global optimality of the Hohmann transfer in the class of two-impulse transfers were first supplied by Lawden [9,10], using the calculus of variations, and Barrar [11]. Then Moyer [12] demonstrated the global optimality of Hohmann and bielliptic transfers from a circular to an elliptic orbit without restrictions on the number of impulses. Still later, Marec [13] employed a hodograph analysis to prove the optimality of the Hohmann transfer, and Battin [14] achieved the same result by using Lagrange multipliers. Most recently, Palmore [15], Prussing [16], and Yuan and Matsushima [17] presented elementary proofs of the global optimality of the Hohmann transfer in the class of two-impulse transfers. In his valuable paper, Hazelrigg [18] described a quite interesting approach to the analysis of global optimal transfers without any limitation on the number of impulses. His method was based on the use of Green's theorem and led to results of a global nature regarding impulsive transfers involving any kind of Keplerian trajectory.

In all of the preceding research, as well as in this study, the initial and final trajectories are specified through their specific energy and angular momentum only. The total time required for the transfer is assumed to be unspecified, as is the orientation of the initial and final coplanar trajectories (time-open, angle-open transfers).

The fundamental characteristics of optimal impulsive trajectories are stated by the primer vector theory, which was developed by Lawden [9,10] and is concerned with the application of the first-order necessary conditions for optimality (arising from the calculus of variation) to space trajectories. Conditions on the primer, which represents the adjoint variable conjugated to the velocity vector, can be used to describe an optimal trajectory, either with finite-thrust periods or impulses. The primer vector yields the direction and the position of the impulsive changes of velocity, which must occur

Received 18 April 2008; revision received 15 December 2008; accepted for publication 19 December 2008. 

*Research Assistant, Scuola di Ingegneria Aerospaziale; mauro.pontani@uniroma1.it.

tangentially at the apse points of a Keplerian arc. Lawden [9,10,19] also conjectured the optimality of a specific type of singular, finite-thrust trajectory, the so-called Lawden's spiral. However, if no constraint holds for the thrust level, Lawden's spiral turns out to be nonoptimal, as demonstrated by several researchers [20–24]. This means that a locally optimal trajectory is unequivocally composed of coasting (null-thrust, Keplerian) arcs, separated by impulsive changes of velocity, which are to be applied tangentially at the apse points. These arguments suffice to prove that any finite-thrust trajectory can be equaled or outperformed by an impulsive trajectory. This is the starting point of the present research.

The work that follows proposes a simple, original approach to determine the global optimal impulsive transfers between two coplanar Keplerian trajectories, without any restriction on the number of impulses and with possible constraints on the radius of closest approach or greatest recession (i.e., with a minimum allowed periapse radius and a maximum allowed apoapse radius). Several cases are considered, to take into account all of the possible transfers involving a pair of Keplerian conics as initial and final states. With reference to transfers between two elliptic orbits, this paper is intended to prove that the Hohmann transfer and the bielliptic transfer with the maximum apoapse radius of the intermediate orbits are globally optimal. To do this, a method is employed that uses ordinary calculus in conjunction with a simple graphical procedure aimed at eliminating suboptimal impulses. The graphical procedure described in this paper is analogous to that used by Hazelrigg [18]; nevertheless, all of the fundamental results attained by Hazelrigg through Green's theorem here are simply deduced by using elementary properties of the functions of a single variable. The final choice between Hohmann and bielliptic transfer depends on the orbital parameters (i.e., on the apoapse and periapse radii) of the two orbits. This study addresses a direct analytical method to make this choice in the general case of ellipses of arbitrary periapse and apoapse radii. Global optimal transfers involving elliptic orbits and escape trajectories with possible constraints on the radius of closest approach or greatest recession are also investigated. The objective of this work is to derive a simple, general, analytical approach that leads to the determination of the global optimal transfer between two arbitrary Keplerian trajectories, without any restriction on the number of impulses.

## II. Locally Optimal Orbital Transfers

In the context of angle-open, time-open, planar, impulsive transfers, the following facts are stipulated as theoretical premises for the present research based on previously known results:

1) On Keplerian trajectories (ellipses, parabolas, and hyperbolas), locally optimal finite impulses occur tangentially at apse points: impulses at periapse change the apoapse radius, and impulses at apoapse (of elliptic orbits) change the periapse radius.

2) On hyperbolic and parabolic trajectories, infinitesimal impulses can occur at infinite distance; they change the periapse radius of the conic without modifying its specific energy $E$.

3) Infinitesimal impulses can occur at the periapse of a rectilinear trajectory and are capable of changing the trajectory energy $E$.

Statement 1 summarizes the implications of the primer vector theory applied to impulsive time-open, angle-open transfers. Specifically, property 1 derives from the first-order necessary conditions for optimality and does not lead to any conclusion of a global nature. Statement 2 is demonstrated to hold for hyperbolic trajectories in Appendix A, whereas it is trivial for parabolic trajectories, because the velocity vanishes as the distance from the attracting body tends to infinity. Statement 3 will be proved in this section, by considering the limiting case of an impulse at periapse as the periapse radius tends to zero. Of course, the application of an impulse at periapse of a rectilinear trajectory is concretely infeasible because gravity tends to infinity. However, statement 3 refers to a limiting situation and means that arbitrarily modest impulses at periapse (capable of changing the trajectory energy) can be applied if no constraint holds on the radius of closest approach.

This section is concerned with a convenient representation of Keplerian trajectories and locally optimal transfers (performed through impulsive variations of velocity) as a starting point for all of the subsequent considerations leading to the identification of global optimal transfers. In addition, this section provides the expressions for evaluating the magnitude of the impulses that perform a locally optimal transfer.

A conic trajectory is defined through its periapse radius $r_P$ and through the parameter $X = 1/r_A$:

1) For elliptic orbits, $r_A$ is the apoapse radius.

2) For circular orbits, $r_A = r_P \Rightarrow r_P X = 1$.

3) For parabolic orbits, $r_A \to \infty$, and so $X = 0$.

4) For hyperbolic orbits, $r_A < 0$, and $|r_A|$ represents the periapse distance from the vacant focus.

As a result, in the $r_P$–$X$ plane, each point corresponds to a specific conic. Similar to the previous work made by Hazelrigg [18], optimal orbital transfers can be conveniently represented in this plane. Because of property 1, in the $r_P$–$X$ plane, a sequence of impulsive transfers that satisfy the necessary conditions for (local) optimality may be represented as a cascade of connected horizontal and vertical segments. Moreover, in the same plane, due to property 2, an infinitesimal impulse at infinite distance is associated with a hyperbolic arc. The trajectory (specific) energy $E$ can be expressed as a function of $r_P$ and $X$:

$$E = -\frac{\mu}{2a} = -\frac{\mu}{r_P + r_A} = \frac{-\mu X}{1 + X r_P} \tag{1}$$

Because the application of an infinitesimal impulse at infinite distance does not change $E$, the geometrical locus related to such an impulse is associated with the following equation:

$$\frac{-\mu X}{1 + X r_P} = E_0 = \text{const} \quad \Rightarrow \quad X = -\frac{E_0}{\mu + E_0 r_P} \tag{2}$$

which corresponds to a hyperbola in the $r_P$–$X$ plane, as shown in Fig. 1.

Different regions in the $r_P$–$X$ plane correspond to distinct types of Keplerian trajectories:

1) The region $X > 0$ ($\Leftrightarrow r_A > 0$) corresponds to elliptic orbits.

2) The region $X < 0$ ($\Leftrightarrow r_A < 0$) corresponds to hyperbolic trajectories.

3) The axis $X = 0$ ($\Leftrightarrow r_A \to \infty$) corresponds to parabolic trajectories.

4) The axis $r_P = 0$ corresponds to rectilinear trajectories of the elliptic ($X > 0$), parabolic ($X = 0$), and hyperbolic type ($X < 0$).

5) In the region $r_P > 0$ and $X > 0$, the hyperbolic arc $X = 1/r_P$ corresponds to circular orbits and represents the boundary of all of the feasible states in such a region.

6) In the region $r_P > 0$ and $X < 0$, the hyperbolic arc $X = -1/r_P$ represents the boundary of all of the feasible states, because the condition $X r_P + 1 = 0$ yields an infinite value for the energy $E$.

In addition, impulsive transfers that satisfy the necessary conditions for (local) optimality are represented as follows:

1) In the region of elliptic and circular orbits ($r_P > 0$, $X > 0$, and $r_P X \leq 1$), horizontal segments (impulses at apoapse) and vertical segments (impulses at periapse) represent locally optimal transfers.

2) In the region of hyperbolic trajectories ($r_P > 0$, $X < 0$, and $r_P X > -1$), vertical segments (impulses at periapse) and hyperbolic arcs [infinitesimal impulses at infinite distance, characterized by a constant value for the energy and associated with the relationship (2)] represent locally optimal transfers.

3) On the line ($r_P \geq 0$ and $X = 0$), corresponding to parabolic trajectories, horizontal segments (infinitesimal impulses at infinite distance, characterized by $E_0 = 0$) represent locally optimal transfers.

4) On the line $r_P = 0$, corresponding to rectilinear trajectories, vertical segments (infinitesimal impulses at periapse) represent locally optimal transfers.

5) Starting from the line $r_P = 0$, locally optimal transfers are represented as horizontal segments if $X > 0$ (impulses at apoapse of a

rectilinear trajectory of the elliptic type) or as hyperbolic arcs if $X < 0$ (infinitesimal impulses at infinite distance on a rectilinear trajectory of the hyperbolic type).

Using the vis-viva equation arising from conservation of energy, on a conic trajectory the following expression can be deduced for the velocity magnitude $v$:

$$v = \sqrt{\frac{2\mu}{r} - \frac{\mu}{a}} = \sqrt{2\mu}\sqrt{\frac{1}{r} - \frac{1}{r_P + r_A}} = \sqrt{2\mu}\sqrt{\frac{1}{r} - \frac{X}{r_P X + 1}} \quad (3)$$

This relationship can be used to determine the magnitudes of the tangential impulses to enter or depart a trajectory:

1) Impulses at periapse modify the apoapse radius; the impulse $\Delta v_X$ that changes the initial apoapse radius $r_{AI} = 1/X_I$ to the value $r_{AF} = 1/X_F$ has the following magnitude:

$$\Delta v_X(X_I, X_F) = \sqrt{\frac{2\mu}{r_P}}\left|\sqrt{\frac{1}{1 + r_P X_I}} - \sqrt{\frac{1}{1 + r_P X_F}}\right| \quad (4)$$

2) Impulses at apoapse modify the periapse radius; the impulse $\Delta v_{rP}$ that changes the initial periapse radius $r_{PI}$ to the value $r_{PF}$ has the following magnitude:

$$\Delta v_{rP}(r_{PI}, r_{PF}) = \sqrt{2\mu}\left|X\left[\sqrt{\frac{r_{PF}}{1 + r_{PF}X}} - \sqrt{\frac{r_{PI}}{1 + r_{PI}X}}\right]\right| \quad (5)$$

Each velocity change is parallel to the instantaneous velocity vector and has the same direction if the orbit energy is to be increased or the opposite direction if the orbit energy is to be reduced. In the region $X > 0$, from state I to state F, a possible sequence of 10 impulses that satisfy the necessary conditions for (local) optimality is portrayed in Fig. 2a.

In the region of hyperbolic trajectories ($X < 0$), impulses at periapse modify $X$, and the relationship (4) holds again. In contrast, Eq. (5) is meaningless because no apoapse exists on a hyperbolic orbit. As previously remarked, among hyperbolic trajectories, optimal transfers are thus represented as vertical segments (impulses at periapse) and hyperbolic arcs (infinitesimal impulses at infinite distance). Two possible orbital transfers satisfying the necessary conditions for (local) optimality are portrayed in Fig. 2b.

1) The transfer ABCD is performed through two impulses at periapse, divided by an infinitesimal impulse at infinite distance. As the first impulse at infinity must be unequivocally performed while leaving from the attracting body, the second cannot be performed, and the sequence ABCD turns out to be infeasible.

2) The transfer LMNO is performed through two infinitesimal impulses divided by an impulse at periapse. The first impulse is performed at infinity while approaching the attracting body, and the third is performed at infinity while leaving from it.

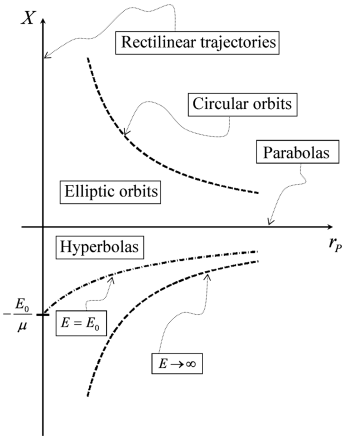


**Fig. 1 Representation of the Keplerian trajectories in the $r_P$–$X$ plane.**

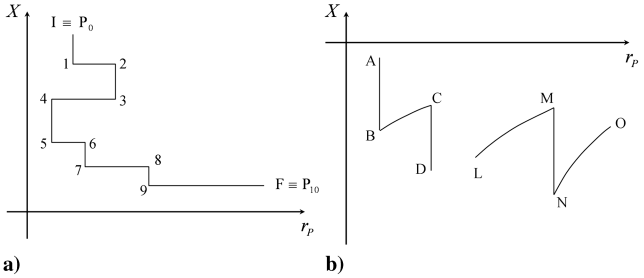


**Fig. 2 Example of locally optimal transfers (represented in the $r_P$–$X$ plane).**

Orbital transfers can involve, at most, two infinitesimal impulses at infinite distance. Transfers similar to that associated with path ABCD of Fig. 2b are infeasible.

Some basic properties concerning (locally) optimal transfers can be easily derived. Using Eqs. (4) and (5), the following property is immediately evident:

$$\begin{aligned} \Delta v_X(X_I, X_F) &= \Delta v_X(X_F, X_I) \quad \text{and} \\ \Delta v_{rP}(r_{PI}, r_{PF}) &= \Delta v_{rP}(r_{PF}, r_{PI}) \end{aligned} \quad (6)$$

That is, the impulse required for changing the initial state (related to the initial orbit) into the final state (related to the final orbit) is the same if the two states are interchanged, provided that the orbital transfers are locally optimal (i.e., they must occur along vertical or horizontal arcs in the $r_P$–$X$ plane). This circumstance implies that the total cost of an optimal orbital transfer can be evaluated regardless of which is the initial and which is the final state.

In addition, using Eq. (4) again, the following additive properties can be easily proved:

$$\Delta v_X(X_I, X_F) = \Delta v_X(X_I, X_1) + \Delta v_X(X_1, X_F) \quad (7)$$

where

$$\begin{cases} X_I < X_1 < X_F & \text{if } X_I < X_F \\ X_F < X_1 < X_I & \text{if } X_F < X_I \end{cases}$$

$$\Delta v_{rP}(r_{PI}, r_{PF}) = \Delta v_{rP}(r_{PI}, r_{P1}) + \Delta v_{rP}(r_{P1}, r_{PF}) \quad (8)$$

where

$$\begin{cases} r_{PI} < r_{P1} < r_{PF} & \text{if } r_{PI} < r_{PF} \\ r_{PF} < r_{P1} < r_{PI} & \text{if } r_{PF} < r_{PI} \end{cases}$$

That is, in terms of total velocity change, any orbital transfer performed by applying two subsequent tangential impulses at periapse (apoapse) is equivalent to the application of a single impulse. By induction, one can deduce that a vertical (horizontal) line can represent a sequence of an arbitrary number of subsequent impulses at periapse (apoapse), the sequence of which is equivalent to applying a single impulse. Finally, using Eq. (4), one obtains

$$\begin{aligned} \lim_{r_P \to 0} \Delta v_X(X_I, X_F) &= \lim_{r_P \to 0}\left\{\sqrt{\frac{2\mu}{r_P}}\left|\frac{1}{1 + r_P X_I}\right.\right. \\ &\left.\left. - \frac{1}{1 + r_P X_F}\right|\left[\sqrt{\frac{1}{1 + r_P X_I}} + \sqrt{\frac{1}{1 + r_P X_F}}\right]^{-1}\right\} \\ &= \lim_{r_P \to 0}\left\{\sqrt{2\mu r_P}|X_F - X_I|\left[\sqrt{\frac{1}{1 + r_P X_I}} + \sqrt{\frac{1}{1 + r_P X_F}}\right]^{-1}\right\} = 0 \\ &\forall\ (X_I, X_F) \end{aligned} \quad (9)$$

That is, in the limit as $r_P \to 0$, the velocity impulse required for changing $X_I$ to the value $X_F$ is zero. This means that on a rectilinear trajectory, an arbitrary modification of the orbit energy $E$ [related to

$X$ through Eq. (1)] can be achieved by means of an infinitesimal impulse at periapse, represented as a vertical segment lying on the axis $r_P = 0$.

## III. Globally Optimal Transfers Between Two Elliptic Orbits

To determine the fundamental features of the global optimal impulsive transfers between two elliptic orbits without any restriction on the number of impulses, globally optimal transfers in the class of two-impulse transfers must first be identified. This goal can be achieved by applying a simple analytical procedure based on ordinary calculus, which leads to the same results achieved by Hazelrigg [18] through Green's theorem. The following elementary properties of continuous differentiable functions of a single variable $\xi$ will be extensively used:

$$\frac{\mathrm{d}f}{\mathrm{d}\xi} > 0 \quad \forall\ \xi \in [\min(\xi_A, \xi_B), \max(\xi_A, \xi_B)] \Rightarrow \begin{cases} f(\xi_B) > f(\xi_A) & \text{if } \xi_B > \xi_A \\ f(\xi_B) < f(\xi_A) & \text{if } \xi_B < \xi_A \end{cases} \tag{10}$$

$$\frac{\mathrm{d}f}{\mathrm{d}\xi} < 0 \quad \forall\ \xi \in [\min(\xi_A, \xi_B), \max(\xi_A, \xi_B)] \Rightarrow \begin{cases} f(\xi_B) < f(\xi_A) & \text{if } \xi_B > \xi_A \\ f(\xi_B) > f(\xi_A) & \text{if } \xi_B < \xi_A \end{cases} \tag{11}$$

In the region $r_P > 0$, $X > 0$, and $r_P X \leq 1$, including all of the possible elliptic orbits, four mutual positions exist for the initial and the final states, corresponding to the terminal[†] orbits, represented as points I and F in Fig. 3. However, as the total cost of an optimal orbital transfer can be evaluated regardless of which is the initial and which is the final state, only the cases portrayed in Figs. 3a and 3b are to be examined.

### A. Case A: $X_F > X_I$, $r_{PF} > r_{PI}$, $I \equiv B$, and $F \equiv D$

In Fig. 3a, the two paths IAF and ICF are compared to prove that

$$\Delta v_{IAF} > \Delta v_{ICF} \Leftrightarrow \Delta v_{IAF} - \Delta v_{ICF} > 0$$

Using Eqs. (4) and (5), one obtains

$$\begin{aligned} \frac{\Delta v_{IAF} - \Delta v_{ICF}}{\sqrt{2\mu}} &= \frac{(\Delta v_{IA} + \Delta v_{AF}) - (\Delta v_{IC} + \Delta v_{CF})}{\sqrt{2\mu}} \\ &= \frac{1}{\sqrt{r_{PI}}}\left[\frac{1}{\sqrt{1 + r_{PI}X_I}} - \frac{1}{\sqrt{1 + r_{PI}X_F}}\right] \\ &+ X_F\left[\sqrt{\frac{r_{PF}}{1 + r_{PF}X_F}} - \sqrt{\frac{r_{PI}}{1 + r_{PI}X_F}}\right] \\ &- \frac{1}{\sqrt{r_{PF}}}\left[\frac{1}{\sqrt{1 + r_{PF}X_I}} - \frac{1}{\sqrt{1 + r_{PF}X_F}}\right] \\ &- X_I\left[\sqrt{\frac{r_{PF}}{1 + r_{PF}X_I}} - \sqrt{\frac{r_{PI}}{1 + r_{PI}X_I}}\right] \end{aligned} \tag{12}$$

Two auxiliary functions are now introduced as

$$\begin{aligned} f_1(r_P) &\triangleq -\frac{1}{\sqrt{r_P}}\left[\frac{1}{\sqrt{1 + r_P X_I}} - \frac{1}{\sqrt{1 + r_P X_F}}\right] \quad \text{and} \\ f_2(X) &\triangleq X\left[\sqrt{\frac{r_{PF}}{1 + r_{PF}X}} - \sqrt{\frac{r_{PI}}{1 + r_{PI}X}}\right] \end{aligned} \tag{13}$$

and Eq. (12) can be rewritten as

[†]The word "terminal," referring to orbits or states, will be used as the equivalent to "initial and final" henceforth.

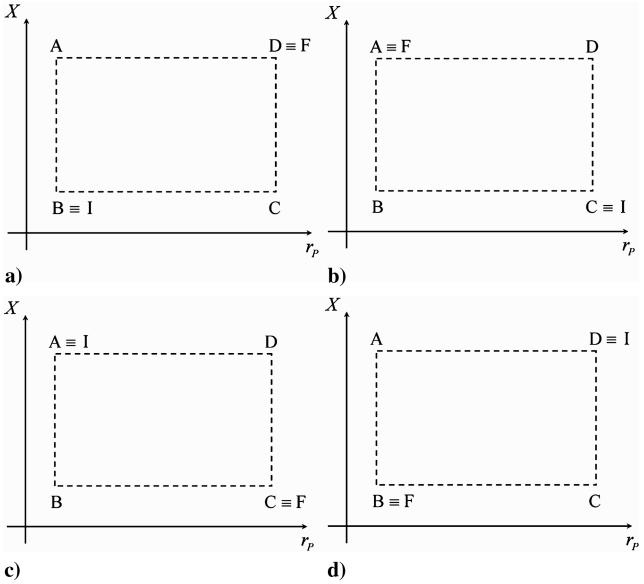


**Fig. 3 Two-impulse transfers between two elliptic orbits (represented in the $r_P$–$X$ plane).**

$$\frac{\Delta v_{IAF} - \Delta v_{ICF}}{\sqrt{2\mu}} = [f_1(r_{PF}) - f_1(r_{PI})] + [f_2(X_F) - f_2(X_I)] \tag{14}$$

What will be demonstrated is that both terms included in the square brackets of Eq. (14) are positive. To do this, the first derivatives of $f_1(r_P)$ and $f_2(X)$ with respect to $r_P$ and $X$ are considered:

$$\frac{\mathrm{d}f_1}{\mathrm{d}r_P} = \frac{1}{2r_P^{3/2}\sqrt{1 + r_P X_I}} - \frac{1}{2r_P^{3/2}\sqrt{1 + r_P X_F}} \tag{15}$$

$$\frac{\mathrm{d}f_2}{\mathrm{d}X} = \frac{2 + r_{PF}X}{2(1 + r_{PF}X)}\sqrt{\frac{r_{PF}}{1 + r_{PF}X}} - \frac{2 + r_{PI}X}{2(1 + r_{PI}X)}\sqrt{\frac{r_{PI}}{1 + r_{PI}X}} \tag{16}$$

Letting

$$\begin{aligned} g_1(X) &\triangleq -\frac{1}{2r_P^{3/2}\sqrt{1 + r_P X}} \quad \text{and} \\ g_2(r_P) &\triangleq \frac{2 + r_P X}{2(1 + r_P X)}\sqrt{\frac{r_P}{1 + r_P X}} \end{aligned} \tag{17}$$

Equations (15) and (16) become

$$\frac{\mathrm{d}f_1}{\mathrm{d}r_P} = g_1(X_F) - g_1(X_I) \quad \text{and} \quad \frac{\mathrm{d}f_2}{\mathrm{d}X} = g_2(r_{PF}) - g_2(r_{PI}) \tag{18}$$

It then follows that

$$\begin{aligned} \frac{\mathrm{d}g_1}{\mathrm{d}X} &= \frac{1}{4\sqrt{r_P}(1 + r_P X)^{3/2}} > 0 \quad \text{and} \\ \frac{\mathrm{d}g_2}{\mathrm{d}r_P} &= \frac{2 - r_P X}{4\sqrt{r_P}(1 + r_P X)^{5/2}} > 0 \quad (\text{as } r_P X \leq 1) \end{aligned} \tag{19}$$

As $X_F > X_I$ and $r_{PF} > r_{PI}$, due to Eq. (10), the relationships (19) imply

$$\frac{\mathrm{d}f_1}{\mathrm{d}r_P} = g_1(X_F) - g_1(X_I) > 0 \quad \text{and} \quad \frac{\mathrm{d}f_2}{\mathrm{d}X} = g_2(r_{PF}) - g_2(r_{PI}) > 0 \tag{20}$$

Again, from Eqs. (10) and (20), one obtains

$$f_1(r_{PF}) - f_1(r_{PI}) > 0 \quad \text{and} \quad f_2(X_F) - f_2(X_I) > 0 \tag{21}$$

and these inequalities finally lead to the desired result:

$$\Delta v_{IAF} > \Delta v_{ICF} \quad \forall\ (I,F) \quad \text{such that} \begin{cases} r_{PF} > r_{PI} & \geq 0 \\ X_F > X_I & \geq 0 \end{cases} \tag{22}$$

Hence, the optimal path from point I to point F is composed of two segments: IC and CF, the former corresponding to an impulse at apoapse, the latter corresponding to an impulse at periapse. In addition, due to the previous considerations about interchangeability of points I and F, the optimal path for the case portrayed in Fig. 3d is composed of the segments IC and CF (corresponding to an impulse at periapse followed by an impulse at apoapse). Figures 4a and 4d illustrate the optimal transfers related to the cases of Figs. 3a and 3d, respectively.

### B. Case B: $X_F > X_I$, $r_{PF} < r_{PI}$, $I \equiv C$, and $F \equiv A$

In Fig. 3b, the two paths IDF and IBF are compared to prove that

$$\Delta v_{IDF} > \Delta v_{IBF} \Leftrightarrow \Delta v_{IDF} - \Delta v_{IBF} > 0$$

Using Eqs. (4) and (5), one obtains

$$\begin{aligned} \frac{\Delta v_{IDF} - \Delta v_{IBF}}{\sqrt{2\mu}} &= \frac{(\Delta v_{ID} + \Delta v_{DF}) - (\Delta v_{IB} + \Delta v_{BF})}{\sqrt{2\mu}} \\ &= \frac{1}{\sqrt{r_{PI}}}\left[\frac{1}{\sqrt{1 + r_{PI}X_I}} - \frac{1}{\sqrt{1 + r_{PI}X_F}}\right] \\ &+ X_F\left[\sqrt{\frac{r_{PI}}{1 + r_{PI}X_F}} - \sqrt{\frac{r_{PF}}{1 + r_{PF}X_F}}\right] \\ &- \frac{1}{\sqrt{r_{PF}}}\left[\frac{1}{\sqrt{1 + r_{PF}X_I}} - \frac{1}{\sqrt{1 + r_{PF}X_F}}\right] \\ &- X_I\left[\sqrt{\frac{r_{PI}}{1 + r_{PI}X_I}} - \sqrt{\frac{r_{PF}}{1 + r_{PF}X_I}}\right] \end{aligned} \tag{23}$$

Two auxiliary functions are introduced as

$$\begin{aligned} f_1(r_P) &\triangleq \frac{1}{\sqrt{r_P}}\left[\frac{1}{\sqrt{1 + r_P X_F}} - \frac{1}{\sqrt{1 + r_P X_I}}\right] \quad \text{and} \\ f_2(X) &\triangleq X\left[\sqrt{\frac{r_{PI}}{1 + r_{PI}X}} - \sqrt{\frac{r_{PF}}{1 + r_{PF}X}}\right] \end{aligned} \tag{24}$$

and Eq. (23) can be rewritten as

$$\frac{\Delta v_{IDF} - \Delta v_{IBF}}{\sqrt{2\mu}} = [f_1(r_{PF}) - f_1(r_{PI})] + [f_2(X_F) - f_2(X_I)] \tag{25}$$

Also in this case, it will be demonstrated that both terms included in the square brackets of Eq. (25) are positive. To do this, the first derivatives of $f_1(r_P)$ and $f_2(X)$ with respect to $r_P$ and $X$ are considered:

$$\frac{\mathrm{d}f_1}{\mathrm{d}r_P} = \frac{1}{2r_P^{3/2}\sqrt{1 + r_P X_I}} - \frac{1}{2r_P^{3/2}\sqrt{1 + r_P X_F}} \tag{26}$$

$$\frac{\mathrm{d}f_2}{\mathrm{d}X} = \frac{2 + r_{PI}X}{2(1 + r_{PI}X)}\sqrt{\frac{r_{PI}}{1 + r_{PI}X}} - \frac{2 + r_{PF}X}{2(1 + r_{PF}X)}\sqrt{\frac{r_{PF}}{1 + r_{PF}X}} \tag{27}$$

Letting

$$\begin{aligned} g_1(X) &\triangleq -\frac{1}{2r_P^{3/2}\sqrt{1 + r_P X}} \quad \text{and} \\ g_2(r_P) &\triangleq -\frac{2 + r_P X}{2(1 + r_P X)}\sqrt{\frac{r_P}{1 + r_P X}} \end{aligned} \tag{28}$$

Equations (26) and (27) become

$$\frac{\mathrm{d}f_1}{\mathrm{d}r_P} = g_1(X_F) - g_1(X_I) \quad \text{and} \quad \frac{\mathrm{d}f_2}{\mathrm{d}X} = g_2(r_{PF}) - g_2(r_{PI}) \tag{29}$$

Then it follows that

$$\begin{aligned} \frac{\mathrm{d}g_1}{\mathrm{d}X} &= \frac{1}{4\sqrt{r_P}(1 + r_P X)^{3/2}} > 0 \quad \text{and} \\ \frac{\mathrm{d}g_2}{\mathrm{d}r_P} &= \frac{r_P X - 2}{4\sqrt{r_P}(1 + r_P X)^{5/2}} < 0 \quad (\text{as } r_P X \leq 1) \end{aligned} \tag{30}$$

As $X_F > X_I$ and $r_{PF} < r_{PI}$, due to Eqs. (10) and (11), the relationships (30) imply

$$\frac{\mathrm{d}f_1}{\mathrm{d}r_P} = g_1(X_F) - g_1(X_I) > 0 \quad \text{and} \quad \frac{\mathrm{d}f_2}{\mathrm{d}X} = g_2(r_{PF}) - g_2(r_{PI}) > 0 \tag{31}$$

Again, from Eqs. (10) and (31), one obtains

$$f_1(r_{PF}) - f_1(r_{PI}) > 0 \quad \text{and} \quad f_2(X_F) - f_2(X_I) > 0 \tag{32}$$

and these inequalities finally lead to the desired result:

$$\Delta v_{IDF} > \Delta v_{IBF} \quad \forall\ (I,F) \quad \text{such that} \begin{cases} 0 \leq r_{PF} < r_{PI} \\ 0 \leq X_I < X_F \end{cases} \tag{33}$$

Hence, the optimal path from point I to point F is composed of segments IB and BF, the former corresponding to an impulse at apoapse, the latter corresponding to an impulse at periapse. In addition, due to the previous considerations about the interchangeability of points I and F, the optimal path for the case portrayed in Fig. 3c is composed of the segments IB and BF (corresponding to an impulse at periapse followed by an impulse at apoapse). Figures 4b and 4c illustrate the optimal transfers related to the cases of Figs. 3b and 3c, respectively.

This analysis suffices for the identification of the globally optimal impulsive transfer in the class of two-impulse orbital transfers: the *Hohmann transfer*. In addition, it emerges that the terminal ellipses are optimally oriented when they are coaxial and aligned (i.e., with periapses on the same side), as illustrated in Fig. 4. This result is consistent with the considerations made by Ting [7], Hazelrigg [18], and Winn [25].

### C. Multiple-Impulse Transfers

The preceding analysis is extremely useful for achieving conclusions of a global nature regarding impulsive transfers without any restriction on the number of impulses. In fact, with reference to an arbitrary sequence of (local) optimal impulses, such as the one portrayed in Fig. 5, a simple graphical method allows the selection of the global optimal path from point I to point F. The elimination of suboptimal paths in Fig. 5 can be made by taking into account the preceding results in the $r_P$–$X$ plane:

1) From point 1 to point 3, path 123 is outperformed by path 1A3, and so path 123 is eliminated.

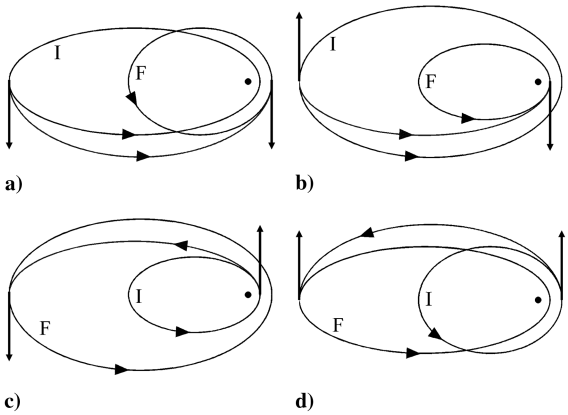


**Fig. 4 Optimal Hohmann transfers from the initial orbit I to the final orbit F.**

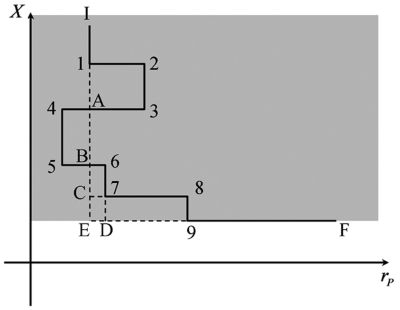


**Fig. 5 Local and global optimal transfers in the shaded region.**

2) Starting from point 3, point 4 is reached passing through point A, but point A is reached directly from point 1, and so path 123A can be eliminated.

3) From point A to point 5, path A45 is outperformed by path AB5, and so A45 is eliminated.

4) Starting from point 5, point 6 is reached passing through point B, but point B is reached directly from point A, and so path A45B can be eliminated.

5) From point B to point 7, path B67 is outperformed by path BC7, and so path B67 is eliminated.

6) From point 7 to point 9, path 789 is outperformed by path 7D9, and so path 789 is eliminated.

7) From point C to point D, path C7D is outperformed by path CED, and so path C7D is eliminated.

Finally, the optimal transfer is composed of five consecutive impulses at periapse (I1, 1A, AB, BC, and CE) followed by three consecutive impulses at apoapse (ED, D9, and 9F). However, due to the additive properties [stated by the relationships (7) and (8)] in terms of total velocity change, the first five impulses are equivalent to applying a single impulse at periapse (IE), whereas the latter three impulses are equivalent to applying a single impulse at apoapse (EF). Therefore, this straightforward graphical method, which can be employed for any arbitrary sequence of (locally optimal) impulses in the shaded region of Fig. 5, leads to the identification of the global optimal transfer among all of the possible transfers (without any restriction on the number of impulses): the *two-impulse Hohmann transfer*.

However, this result holds only in the shaded region shown in Fig. 5 (i.e., if feasible intermediate orbits are assumed to possess an apoapse radius not greater than that of the initial orbit or that of the final orbit):

$$X_B \geq \min\{X_I, X_F\} \tag{34}$$

In fact, the same graphical procedure can be applied to the impulses represented in Fig. 6 (where $X_{\min} = 1/r_A^{(\max)}$ denotes the minimum allowed value for $X$, corresponding to the maximum allowed value of the apoapse radius, $r_A^{(\max)}$):

1) From point 1 to point 3, path 123 is outperformed by path 1A3, and so path 123 is eliminated.

2) Starting from point 3, point 4 is reached passing through point A, but point A is reached directly from point 1, and so path 123A can be eliminated.

3) From point A to point 5, path A45 is outperformed by path AB5, and so path A45 is eliminated.

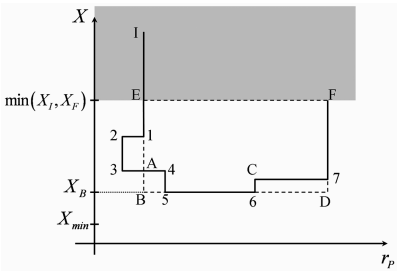


**Fig. 6 Local and global optimal transfers outside the shaded region.**

4) From point 6 to point 7, path 6C7 is outperformed by path 6D7, and so path 6C7 is eliminated.

The optimal transfer is performed through three consecutive impulses at periapse (I1, 1A, and AB), followed by three consecutive impulses at apoapse (B5, 56, and 6D), and, finally, by two impulses at periapse (D7 and 7F). However, due to the additive properties [stated by the relationships (7) and (8)] in terms of total velocity change, such a transfer is equivalent to applying three impulses: the first at periapse (represented as IB), the second at apoapse (represented as BD), and the third at periapse again (represented as DF). Hence, the method leads to the identification of an alternative class of possible global optimal transfers: the *three-impulse bielliptic transfers*; each of them corresponds to a specific value of $X_B$, which is related to the apoapse radius of the intermediate orbit. $X_B$ is constrained to the following range:

$$X_{\min} \leq X_B \leq \min\{X_I, X_F\} \tag{35}$$

The biparabolic transfer is the limiting case of the bielliptic transfer as the midcourse impulse location tends to infinity; that is,

$$X_B^{-1} = r_A^{(\max)} \to \infty \Leftrightarrow X_B = X_{\min} = 0$$

The total velocity change corresponding to each bielliptic transfer, also referred to as the *characteristic velocity* of the transfer, is the sum of the following three terms:

1) Impulse at periapse IB is

$$\Delta v_X(X_I, X_B) = -\sqrt{\frac{2\mu}{r_{PI}}}\left[\sqrt{\frac{1}{1 + r_{PI}X_I}} - \sqrt{\frac{1}{1 + r_{PI}X_B}}\right] \tag{36}$$

2) Impulse at apoapse BD is

$$\Delta v_{rP}(r_{PI}, r_{PF}) = X_B\sqrt{2\mu}\left|\sqrt{\frac{r_{PF}}{1 + r_{PF}X_B}} - \sqrt{\frac{r_{PI}}{1 + r_{PI}X_B}}\right| \tag{37}$$

3) Impulse at periapse DF is

$$\Delta v_X(X_B, X_F) = \sqrt{\frac{2\mu}{r_{PF}}}\left[\sqrt{\frac{1}{1 + r_{PF}X_B}} - \sqrt{\frac{1}{1 + r_{PF}X_F}}\right] \tag{38}$$

Note that Hohmann and biparabolic transfers can be found as special cases from the preceding expressions (36–38):

1) The Hohmann transfer corresponds to $X_B = \min\{X_I, X_F\}$:

a) If $X_I < X_F$, then $\Delta v_X(X_I, X_B) = 0$ [from Eq. (36)].

b) If $X_F < X_I$, then $\Delta v_X(X_B, X_F) = 0$ [from Eq. (38)].

2) The biparabolic transfer corresponds to $X_B = X_{\min} = 0$; from Eq. (37), it follows that $\Delta v_{rP}(r_{PI}, r_{PF}) = 0$ and the midcourse impulse becomes of infinitesimal size.

Equations (36–38) identify a specific class of transfers, including Hohmann and all of the bielliptic transfers. The graphical method employed for determining the optimal path in Fig. 6 yields the same result for any value of $X_B$ in the range of $X_{\min} \leq X_B \leq \min\{X_I, X_F\}$. Hence, the method at hand cannot make a comparison between the total costs corresponding to paths IBDF and IEF of Fig. 6. This is due to the fact that the inequality

$$\Delta v_X(X_E, X_B) + \Delta v_{rP}(r_{PB}, r_{PD}) + \Delta v_X(X_D, X_F) \stackrel{?}{<} \Delta v_{rP}(r_{PE}, r_{PF}) \tag{39}$$

cannot be established through the preceding results on two-impulse transfers. As a consequence, the method cannot be used to choose the optimal path between IBDF and IEF. However, this final choice is addressed in the next section through an original general approach that is capable of identifying the global optimal transfer between two elliptic orbits of arbitrary periapse and apoapse radii.

### D. Hohmann Transfer Versus Bielliptic Transfer

The global optimal transfer between two elliptic orbits belongs to the class of three-impulse transfers for which the magnitudes are

given by Eqs. (36–38). For specified values of $r_{PI}$, $X_I$, $r_{PF}$, and $X_F$, the globally optimal transfer corresponds to the optimal choice of $X_B$, which is related to the apoapse radius of the intermediate orbit (i.e., to the midcourse impulse location). To address this issue, the following dimensionless auxiliary variables are introduced:

$$\alpha_{\min} \triangleq r_{PI}X_{\min}, \qquad \alpha_I \triangleq r_{PI}X_I, \qquad \alpha_F \triangleq r_{PI}X_F$$
$$\alpha_B \triangleq r_{PI}X_B, \qquad \beta \triangleq \frac{r_{PF}}{r_{PI}} \tag{40}$$

These variables are included in the following ranges:

$$0 \le \alpha_B = r_{PI}X_B \le r_{PI}\min\{X_I, X_F\} \le r_{PI}X_I \le 1 \quad \text{and} \quad \beta > 0 \tag{41}$$

Moreover, the following inequalities hold:

$$X_B \le \min\{X_I, X_F\} \le X_F \Rightarrow \alpha_B \le \alpha_F \tag{42}$$

$$X_F r_{PF} \le 1 \Rightarrow \alpha_F = r_{PI}X_F = \frac{r_{PF}}{\beta}X_F \le \frac{1}{\beta} \tag{43}$$

Equations (42) and (43) imply

$$\alpha_B \le \alpha_F \le \frac{1}{\beta} \quad \Rightarrow \quad \alpha_B\beta \le 1 \tag{44}$$

Using the preceding definitions (40), the relationships (36–38) can be rewritten as follows:

$$\Upsilon_1(\alpha_I, \alpha_B) \triangleq \frac{\Delta v_X(X_I, X_B)}{v_{\text{ref}}} = \sqrt{\frac{1}{1+\alpha_B}} - \sqrt{\frac{1}{1+\alpha_I}} \tag{45}$$

$$\Upsilon_2(\alpha_B, \beta) \triangleq \frac{\Delta v_{rP}(r_{PB}, r_{PD})}{v_{\text{ref}}} = \alpha_B\left|\sqrt{\frac{\beta}{1+\beta\alpha_B}} - \sqrt{\frac{1}{1+\alpha_B}}\right| \tag{46}$$

$$\Upsilon_3(\alpha_B, \alpha_F, \beta) \triangleq \frac{\Delta v_X(X_D, X_F)}{v_{\text{ref}}} = \frac{1}{\sqrt{\beta}}\left[\sqrt{\frac{1}{1+\beta\alpha_B}} - \sqrt{\frac{1}{1+\beta\alpha_F}}\right] \tag{47}$$

where $v_{\text{ref}} \triangleq \sqrt{2\mu/r_{PI}}$. Hence, a generic transfer corresponding to the value $\alpha_B$ has the following (normalized) cost $W$:

$$W(\alpha_I, \alpha_B, \alpha_F, \beta) = \Upsilon_1(\alpha_I, \alpha_B) + \Upsilon_2(\alpha_B, \beta) + \Upsilon_3(\alpha_B, \alpha_F, \beta) \tag{48}$$

Two transfers are now compared: the first, denoted with superscript 1, is the transfer with maximum apoapse radius for the intermediate orbit (i.e., $\alpha_B = \alpha_{\min}$), and the second, denoted with superscript 2, is a generic three-impulse transfer (with $\alpha_{\min} \le \alpha_B \le \min\{\alpha_I, \alpha_F\}$). The following function $Z$ is defined as the difference of the two related costs:

$$\begin{aligned} Z(\alpha_{\min}, \alpha_I, \alpha_B, \alpha_F, \beta) &\triangleq W^{(1)}(\alpha_I, \alpha_{\min}, \alpha_F, \beta) \\ &- W^{(2)}(\alpha_I, \alpha_B, \alpha_F, \beta) = \sqrt{\frac{1}{1+\alpha_{\min}}} - \sqrt{\frac{1}{1+\alpha_B}} \\ &+ \frac{1}{\sqrt{\beta}}\left[\sqrt{\frac{1}{1+\beta\alpha_{\min}}} - \sqrt{\frac{1}{1+\beta\alpha_B}}\right] + \alpha_{\min}\left|\sqrt{\frac{\beta}{1+\beta\alpha_{\min}}}\right. \\ &\left. - \sqrt{\frac{1}{1+\alpha_{\min}}}\right| - \alpha_B\left|\sqrt{\frac{\beta}{1+\beta\alpha_B}} - \sqrt{\frac{1}{1+\alpha_B}}\right| \end{aligned} \tag{49}$$

Inspection of the right-hand side of Eq. (49) reveals that $Z$ is independent of $\alpha_I$ and $\alpha_F$: $Z = Z(\alpha_{\min}, \alpha_B, \beta)$. The following property of $Z$ represents an immediate consequence of its definition:

$$Z(\alpha_{\min}, \alpha_B, \beta)\begin{cases} <0 & \Leftrightarrow \text{ transfer 1 has a lower cost than transfer 2} \\ >0 & \Leftrightarrow \text{ transfer 2 has a lower cost than transfer 1} \end{cases} \tag{50}$$

Therefore, the bielliptic transfer with the maximum apoapse radius of the intermediate orbit is the global optimal transfer if $Z < 0$. However, the optimal value of $\alpha_B$ (i.e., of $X_B$) remains to be determined if $Z > 0$. By definition, this optimal value $\alpha_B^*$ minimizes $W^{(2)}(\alpha_I, \alpha_B, \alpha_F, \beta)$:

$$\alpha_B^* = \arg\min_{\alpha_B}\{W^{(2)}(\alpha_I, \alpha_B, \alpha_F, \beta)\} \quad \text{if } Z(\alpha_{\min}, \alpha_B, \beta) > 0 \tag{51}$$

The function $W^{(2)}$ is positive definite, and so

$$\alpha_B^* = \arg\min_{\alpha_B}\{W^{(2)}(\alpha_I, \alpha_B, \alpha_F, \beta)\} = \arg\max_{\alpha_B}\{-W^{(2)}(\alpha_I, \alpha_B, \alpha_F, \beta)\} \tag{52}$$

In addition, $W^{(1)}$ is independent of $\alpha_B$; as a consequence,

$$\alpha_B^* = \arg\max_{\alpha_B}\{W^{(1)}(\alpha_I, \alpha_{\min}, \alpha_F, \beta) - W^{(2)}(\alpha_I, \alpha_B, \alpha_F, \beta)\} \tag{53}$$

Using the definition given in Eq. (49), Eq. (53) finally reduces to

$$\alpha_B^* = \arg\max_{\alpha_B}\{Z(\alpha_{\min}, \alpha_B, \beta)\} \quad \text{if } Z(\alpha_{\min}, \alpha_B, \beta) > 0 \tag{54}$$

That is, the optimal value $\alpha_B^*$ is such that $Z$ is maximized wherever $Z > 0$. To determine $\alpha_B^*$, the partial derivative $\partial Z/\partial\alpha_B$ can be considered. This derivative has two distinct expressions (for $\beta < 1$ and $\beta > 1$), both independent of $\alpha_{\min}$:

$$\frac{\partial Z}{\partial\alpha_B} = \frac{1}{2}\left[\frac{3+\alpha_B}{(1+\alpha_B)^{\frac{3}{2}}} - \left(\frac{\beta}{1+\alpha_B\beta}\right)^{\frac{1}{2}}\right] \quad \text{if } \beta > 1 \tag{55}$$

$$\frac{\partial Z}{\partial\alpha_B} = \frac{1}{2}\left[\frac{\beta^{1/2}(3+\alpha_B\beta)}{(1+\alpha_B\beta)^{\frac{3}{2}}} - \frac{1}{(1+\alpha_B)^{\frac{1}{2}}}\right] \quad \text{if } \beta < 1 \tag{56}$$

If $\beta > 1$, then $\partial Z/\partial\alpha_B \ge 0$ yields

$$\alpha_B^2(3\beta+1) + 6\alpha_B(\beta+1) + 9 - \beta \ge 0 \tag{57}$$

In the region of interest ($0 \le \alpha_B \le 1$, $\beta > 1$, and $\alpha_B\beta \le 1$), Eq. (57) leads to the following inequality:

$$\alpha_B \ge \frac{-3(\beta+1) + 2\sqrt{\beta(3\beta-2)}}{3\beta+1} \tag{58}$$

which corresponds to the region of the $\alpha_B$–$\beta$ plane to the right of the curve portrayed in Fig. 7a. If $\beta < 1$, then $\partial Z/\partial\alpha_B \ge 0$ yields

$$\alpha_B^2(3\beta^2+\beta^3) + 6\alpha_B(\beta^2+\beta) + 9\beta - 1 \ge 0 \tag{59}$$

In the region of interest ($0 \le \alpha_B \le 1$ and $0 \le \beta \le 1$), Eq. (59) leads to the following inequality:

$$\alpha_B \ge \frac{-3(\beta+1) + 2\sqrt{3-2\beta}}{\beta(3+\beta)} \tag{60}$$

which corresponds to the region of the $\alpha_B$–$\beta$ plane above the curve portrayed in Fig. 7b. What will be demonstrated is that the function $Z$ increases monotonically with respect to $\alpha_B$ (i.e., $\partial Z/\partial\alpha_B > 0$) for any pair of values $(\alpha_B, \beta)$ such that $Z > 0$ (i.e., for any point of the $\alpha_B$–$\beta$ plane at which $Z > 0$). In the $\alpha_B$–$\beta$ plane, the equations corresponding to the inequalities (58) and (60) represent the loci in which $\partial Z/\partial\alpha_B = 0$. The expressions of $\beta$ as a function of $\alpha_B$ over the curves $\partial Z/\partial\alpha_B = 0$, henceforth denoted with $\tilde{\beta} = \tilde{\beta}(\alpha_B)$, are particularly useful to evaluate whether $Z > 0$ or $Z < 0$ over these curves. From Eqs. (58) and (60), one obtains

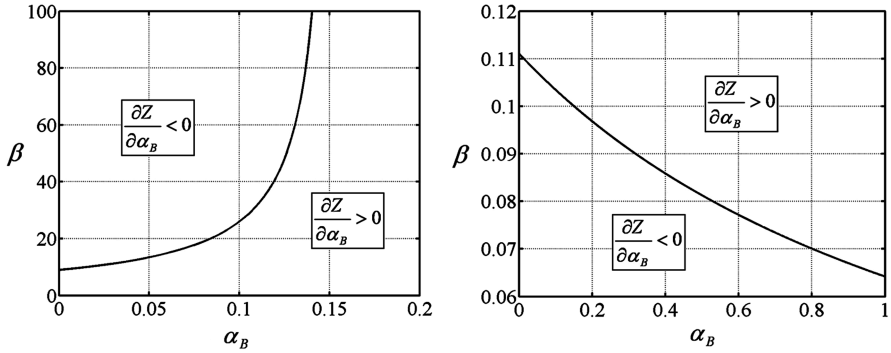


a) b)

**Fig. 7 Curves associated with $(\partial Z/\partial \alpha_B) = 0$.**

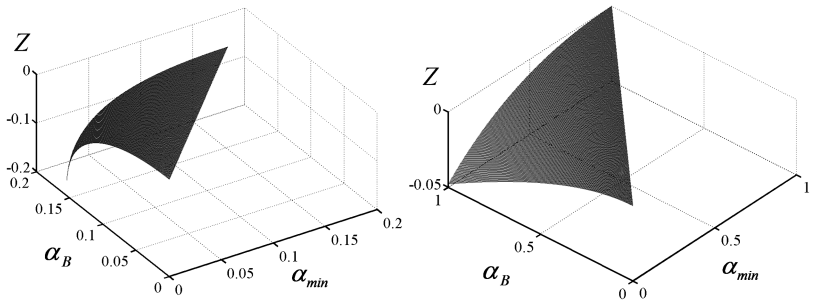


a) b)

**Fig. 8 Function $Z(\alpha_{\min}, \alpha_B, \tilde{\beta}(\alpha_B)) = Z(\alpha_{\min}, \alpha_B)$ evaluated over the curves $(\partial Z/\partial \alpha_B) = 0$.**

$$\tilde{\beta} = -\frac{(\alpha_B + 3)^2}{3\alpha_B^2 + 6\alpha_B - 1} \quad \text{if } \tilde{\beta} > 1 \tag{61}$$

$$\tilde{\beta}^3 \alpha_B^2 + \tilde{\beta}^2(3\alpha_B^2 + 6\alpha_B) + 6\tilde{\beta}\alpha_B + 9\tilde{\beta} - 1 = 0 \quad \text{if } \tilde{\beta} < 1 \tag{62}$$

The right-hand side of Eq. (61) tends to infinity as $\alpha_B \to (2/\sqrt{3}) - 1 \approx 0.155$. One of the three solutions of Eq. (62) (not reported for the sake of brevity) corresponds to the curve illustrated in Fig. 7b.

Using the expressions $\tilde{\beta} = \tilde{\beta}(\alpha_B)$, the function $Z(\alpha_{\min}, \alpha_B, \beta)$ can be evaluated over the curves $\partial Z/\partial \alpha_B = 0$. In this context, $Z$ becomes a function of $\alpha_{\min}$ and $\alpha_B$ only:

$$Z(\alpha_{\min}, \alpha_B, \tilde{\beta}(\alpha_B)) = Z(\alpha_{\min}, \alpha_B)$$

The ranges in which $\alpha_{\min}$ and $\alpha_B$ vary are different in the regions $\tilde{\beta} > 1$ and $\tilde{\beta} < 1$:

$$\tilde{\beta} > 1\text{: } 0 \le \alpha_{\min} < \frac{2}{\sqrt{3}} - 1 \quad \text{and} \quad \alpha_{\min} \le \alpha_B < \frac{2}{\sqrt{3}} - 1 \tag{63}$$

$$\tilde{\beta} < 1\text{: } 0 \le \alpha_{\min} \le 1 \quad \text{and} \quad \alpha_{\min} \le \alpha_B \le 1 \tag{64}$$

The surfaces corresponding to $Z(\alpha_{\min}, \alpha_B)$ are illustrated in Figs. 8a and 8b, which refer to $\tilde{\beta} > 1$ and $\tilde{\beta} < 1$, respectively. In both cases, $Z$ turns out to be negative in the regions defined by Eqs. (63) and (64). This means that $Z < 0$ over the curves $\partial Z/\partial \alpha_B = 0$; hence, the region in which $Z > 0$ is unequivocally included in the region in which $\partial Z/\partial \alpha_B > 0$. As a consequence,

$$\frac{\partial Z}{\partial \alpha_B} > 0 \quad \forall\ (\alpha_B, \beta) \quad \text{such that } Z > 0 \tag{65}$$

That is, with respect to $\alpha_B$, the function $Z$ is monotonically increasing for any pair of values $(\alpha_B, \beta)$ such that $Z > 0$. This property holds regardless of the value of $\beta > 0$. As a result, $Z$ is maximized when $\alpha_B$ assumes its maximum value: that is, $\alpha_B^* = \min(\alpha_I, \alpha_F)$.

In summary, the globally optimal value $\alpha_B^*$, which identifies the globally optimal transfer, is

$$\alpha_B^* = \begin{cases} \alpha_{\min} & \text{if } Z < 0 \leftrightarrow \text{bielliptic transfer with } r_A^{(\max)} \text{for the intermediate orbit} \\ \min(\alpha_I, \alpha_F) & \text{if } Z > 0 \leftrightarrow \text{ Hohmann transfer} \end{cases} \tag{66}$$

Therefore, the curves $Z = 0$ in the $\alpha_B$–$\beta$ plane, which can be plotted once $\alpha_{\min}$ is specified, separate the regions in which the Hohmann transfer is globally optimal from the regions in which the bielliptic transfer with the maximum apoapse radius of the intermediate orbit is globally optimal. The final choice between these two transfers turns out to depend only on three parameters: $\beta$, $\min\{\alpha_I, \alpha_F\}$, and $\alpha_{\min}$ (i.e., the ratios $r_{PF}/r_{PI}$, $\max\{r_{AI}/r_{PI}, r_{AF}/r_{PI}\}$, and $r_A^{(\max)}/r_{PI}$). A schematic illustration of the curves $Z = 0$ (represented as solid lines) is portrayed in Fig. 9. With reference to distinct values of $\alpha_{\min}$, several curves corresponding to $Z = 0$ are shown in Figs. 10a and 10b, corresponding to cases $\beta > 1$ and $\beta < 1$, respectively. For each curve, the value of $\alpha_{\min}$ is reported in the respective inset.

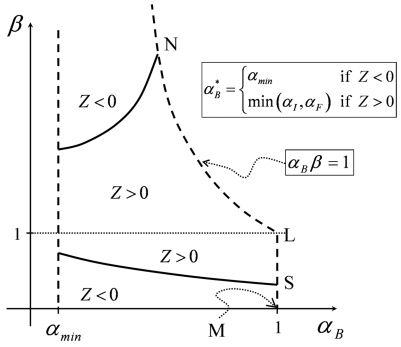


**Fig. 9 Regions of global optimality of Hohmann and bielliptic transfers.**

From a practical point of view, the following steps lead to the optimal choice of $\alpha_B$:

1) Given $r_A^{(\max)}$ and $r_{PI}, \alpha_{\min}$ is calculated and one obtains a graphic similar to that of Fig. 9.

2) Given $r_{PF}, X_I$, and $X_F$, the auxiliary variables $\beta, \alpha_I$, and $\alpha_F$ are calculated.

3) Let $\alpha_B^* = \min\{\alpha_I, \alpha_F\}$:

a) If $Z(\alpha_{\min}, \alpha_B^*, \beta) > 0$ [i.e., if the point $(\alpha_B^*, \beta)$ belongs to the region in which $Z > 0$], then the Hohmann transfer is globally optimal, and one concludes that $\alpha_B^* = \min\{\alpha_I, \alpha_F\}$ (i.e., $X_B^* = \min\{X_I, X_F\}$).

b) If $Z(\alpha_{\min}, \alpha_B^*, \beta) < 0$ [i.e., if the point $(\alpha_B^*, \beta)$ belongs to the region in which $Z < 0$], then the bielliptic transfer with maximum apoapse radius of the intermediate orbit is globally optimal, and one concludes that $\alpha_B^* = \alpha_{\min}$ (i.e., $X_B^* = X_{\min}$).

As previously remarked, the biparabolic transfer is the limiting case as the midcourse impulse location tends to infinity: that is,

$$r_A^{(\max)} \to \infty \Leftrightarrow X_{\min} = 0 \Leftrightarrow \alpha_{\min} = 0$$

The method described in this section includes previous results regarding optimal transfers between two circular orbits as special cases. Circular orbits are such that

$$r_{PI} = r_{AI} = \frac{1}{X_I} \triangleq R_I \quad \text{and} \quad r_{PF} = r_{AF} = \frac{1}{X_F} \triangleq R_F \tag{67}$$

Hence, it follows that $\beta = R_F/R_I$. Two cases must be distinguished again:

1) In the first case, $R_F > R_I$ (i.e., $\beta = R_F/R_I > 1$). As $X_F < X_I$,

$$\alpha_B^* = \min\{\alpha_I, \alpha_F\} = \alpha_F = r_{PI}X_F = \frac{R_I}{R_F} = \frac{1}{\beta} \quad \text{if } Z > 0 \tag{68}$$

Hence, in the $\alpha_B$–$\beta$ plane, the geometrical locus related to transfers between circular orbits (with $R_F > R_I$) is the hyperbola corresponding to $\alpha_B^*\beta = 1$, which is represented as a dashed curve in Fig. 9. If $X_{\min} = 0$ (i.e., $\alpha_{\min} = 0$), one obtains the following well-known result concerning exterior biparabolic transfers:

a) The Hohmann transfer is globally optimal if $1 < \beta < \beta_A$, where $\beta_A$ is the value of $\beta$ at point A of Fig. 10a; it follows that $\beta_A \approx 11.939$.

b) The biparabolic transfer is globally optimal if $\beta > \beta_A$.

Even though it is not reported, for the sake of brevity, an analytical expression of $\beta_A$ exists, because $\beta_A$ represents one of the roots of the following third-degree equation, derived in Appendix B:

$$\beta^3 - \beta^2(7 + 4\sqrt{2}) + \beta(3 + 4\sqrt{2}) - 1 = 0 \tag{69}$$

2) In the second case, $R_F < R_I$ (i.e., $\beta = R_F/R_I < 1$). As $X_F > X_I$,

$$\alpha_B^* = \min\{\alpha_I, \alpha_F\} = \alpha_I = r_{PI}X_I = 1 \quad \text{if } Z > 0 \tag{70}$$

Hence, in the $\alpha_B$–$\beta$ plane, the geometrical locus related to transfers between circular orbits (with $R_F < R_I$) is the segment corresponding to $\alpha_B^* = 1$ $(0 < \beta < 1)$, which is represented as a dashed line (LM) in Fig. 9. If $X_{\min} = 0$ (i.e., $\alpha_{\min} = 0$), one obtains the following well-known result regarding interior biparabolic transfers:

a) The Hohmann transfer is globally optimal if $\beta_B < \beta < 1$, where $\beta_B$ is the value of $\beta$ at point B of Fig. 10b; it follows that $\beta_B \approx 0.08376$.

b) The biparabolic transfer is globally optimal if $\beta < \beta_B$.

Also in this case, an analytical expression of $\beta_B$ exists, because $\beta_B$ represents one of the roots of the following equation, derived again in Appendix B:

$$\beta^3 - \beta^2(3 + 4\sqrt{2}) + \beta(7 + 4\sqrt{2}) - 1 = 0 \tag{71}$$

If the generic $\beta_1$ is a root of Eq. (69), then the value $1/\beta_1$ is a root of Eq. (71): this property can be easily verified by letting $\beta = 1/\beta_1$ in Eq. (71), under the assumption that $\beta_1$ satisfies Eq. (69). This circumstance implies that the two values $\beta_A$ and $\beta_B$ are reciprocal (i.e., $\beta_A\beta_B = 1$).

With reference to Fig. 9, if $\alpha_{\min}$ increases (i.e., if $r_A^{(\max)}$ decreases), the point N moves upward along the hyperbola $\alpha_B\beta = 1$. The limiting situation is illustrated in Fig. 11 and corresponds to $\alpha_{\min} = 1/\beta_N^{(\max)} \approx 0.06418$: if $\alpha_{\min} > 1/\beta_N^{(\max)}$ all of the points belonging to the region $\alpha_B \geq \alpha_{\min}$, $\beta > 1$, and $\alpha_B\beta \leq 1$ are such that $Z > 0$. Thus, the Hohmann transfer is unequivocally globally optimal if

$$\alpha_{\min} = r_{PI}X_{\min} = \frac{r_{PI}}{r_A^{(\max)}} > \frac{1}{\beta_N^{(\max)}} \Rightarrow \frac{r_A^{(\max)}}{r_{PI}} < \beta_N^{(\max)} \tag{72}$$

regardless of the remaining data of the initial and final orbits (provided that $\beta > 1$).

Conversely, $\beta_N^{(\max)}(\approx 15.582)$ identifies the maximum meaningful value of $\beta$ for which $Z$ vanishes. This implies that in the region $\alpha_B \geq \alpha_{\min}$, $\beta > 1$, and $\alpha_B\beta \leq 1$, the bielliptic transfer is unequivocally globally optimal if

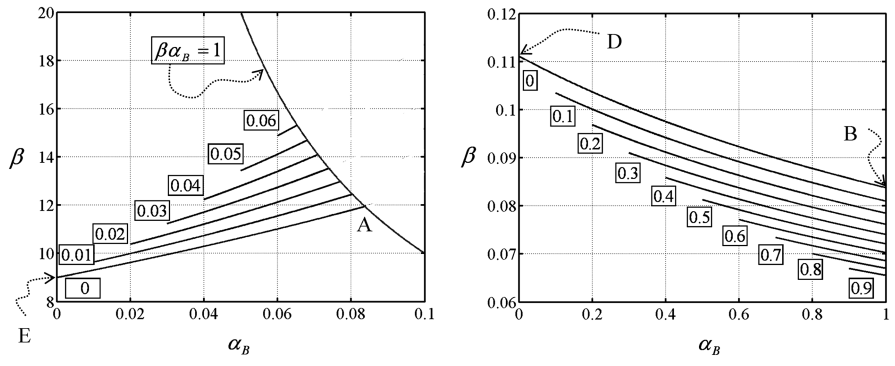


**Fig. 10 Curves associated with $Z = 0$ for different values of $\alpha_{\min}$ (in the insets).**

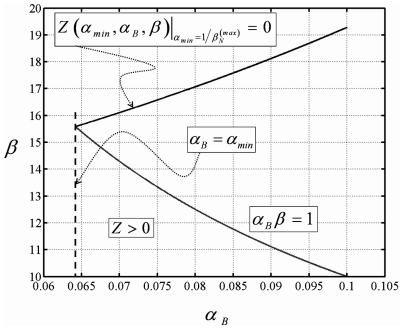


**Fig. 11 Curves associated with $Z = 0$ and $\alpha_B \beta = 1$ in the limiting case $\alpha_{\min} = 1/\beta_N^{(\max)}$.**

$$\beta > \beta_N^{(\max)} \tag{73}$$

regardless of the remaining data of the initial and final orbits, provided that $(r_A^{(\max)}/r_{PI}) > \beta_N^{(\max)}$. This result is well known for circular orbits [26] and is proven here to hold for the more general case of elliptic orbits of arbitrary periapse and apoapse radii. The value $\beta_N^{(\max)}$ represents one of the roots of the following third-degree equation, derived in Appendix B:

$$\beta^3 - 15\beta^2 - 9\beta - 1 = 0 \tag{74}$$

In addition, with reference to Fig. 9, the value of $\beta$ in $S$, $\beta_S$, tends to $\beta_S^{(\min)}$ in the limiting situation as $\alpha_{\min} \to 1$. It follows that $\beta_S^{(\min)} \approx 0.06418$ and one can conclude that an interior biellipticic transfer is unequivocally globally optimal if $\beta < \beta_S^{(\min)}$, regardless of the remaining data of the initial and final orbits. The value $\beta_S^{(\min)}$ represents one of the roots of the following third-degree equation, derived again in Appendix B:

$$\beta^3 + 9\beta^2 + 15\beta - 1 = 0 \tag{75}$$

If the generic $\beta_2$ is a root of Eq. (74), then the value $1/\beta_2$ is a root of Eq. (75). This property can be verified by letting $\beta = 1/\beta_2$ in Eq. (75), under the assumption that $\beta_2$ satisfies Eq. (74). This circumstance implies that the two values $\beta_N^{(\max)}$ and $\beta_S^{(\min)}$ are reciprocal (i.e., $\beta_N^{(\max)} \beta_S^{(\min)} = 1$).

Finally, from an inspection of Fig. 10, it emerges that the biellipticic transfer is never optimal if $\beta_D < \beta < \beta_E$, where $\beta_D$ and $\beta_E$ are the values of $\beta$ at points D and E of Figs. 10b and 10a, respectively. These two values represent, respectively, the maximum and the minimum value of $\beta$ over the curves $Z(\alpha_{\min} = 0, \alpha_B, \beta) = 0$, which constitute the geometrical loci in which the interior and exterior biparabolic transfers have the same cost as the Hohmann transfer. In Appendix B, the two values $\beta_D$ and $\beta_E$ are derived analytically and turn out to be $\beta_D = 1/9 \approx 0.1111$ and $\beta_E = 9$. Thus far, to the author's knowledge, the latter value was found only numerically in a previous work by Marchal [27].

Figure 12 summarizes the major results achieved in this section. The method described for selecting the global optimal transfer can be employed whether $\beta_S^{(\min)} < \beta < \beta_D$ or $\beta_E < \beta < \beta_N^{(\max)}$ and becomes unnecessary if $0 < \beta < \beta_S^{(\min)}$, $\beta_D < \beta < \beta_E$, or $\beta > \beta_N^{(\max)}$, when the global optimal transfer is unequivocally either the Hohmann transfer (if $\beta_D < \beta < \beta_E$) or the biellipticic transfer with the greatest radius of recession from the attracting body (if $0 < \beta < \beta_S^{(\min)}$ or $\beta > \beta_N^{(\max)}$).

## IV. Globally Optimal Transfers Between Two Hyperbolic Trajectories

As mentioned in Sec. II, in the region of hyperbolic trajectories ($X < 0$), two types of locally optimal impulses exist:

1) Impulses at periapse are capable of changing $X$ (and therefore the trajectory energy $E$) and are represented as vertical segments in the $r_P$–$X$ plane.

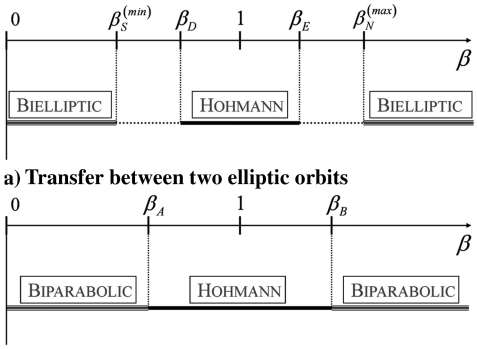


**a) Transfer between two elliptic orbits**




**b) Transfer between two circular orbits**

**Fig. 12 Globally optimal transfers as a function of $\beta$.**

2) Infinitesimal impulses at infinite distance correspond to hyperbolic arcs of constant energy in the $r_P$–$X$ plane.

As previously stated, orbital transfers between hyperbolic trajectories can involve, at most, two infinitesimal impulses at infinite distance, separated by an impulse at periapse, because transfers similar to that corresponding to the sequence ABCD of Fig. 2b are infeasible. With reference to Fig. 13, the determination of the global optimal transfer between two hyperbolic trajectories (represented as points I and F) is equivalent to the identification of the optimal impulse at periapse that allows changing the trajectory energy from the value $E_I$ to $E_F$. This is due to the fact that, starting from point I, the points located on the same hyperbolic arc (i.e., points H, A, and E in Fig. 13) can be reached by means of infinitesimal impulses (without any additional cost). Hence, to determine the globally optimal transfer from point I to point F, only the optimal location of the periapse impulse needs to be found. It will be demonstrated that the globally optimal transfer between two hyperbolic trajectories requires the application of a finite impulse at the minimum allowed periapse radius, denoted with $r_P^{(\min)}$. To do this, the costs associated with two generic segments AB and EG (portrayed in Fig. 13), such that $r_{PE} > r_{PA}$, can be compared. From Eq. (4), one obtains

$$\Delta v_{AB} = \sqrt{\frac{2\mu}{r_{PA}}}\left[\sqrt{\frac{1}{1 + r_{PA}X_A}} - \sqrt{\frac{1}{1 + r_{PA}X_B}}\right] \quad \text{and}$$
$$\Delta v_{EG} = \sqrt{\frac{2\mu}{r_{PE}}}\left[\sqrt{\frac{1}{1 + r_{PE}X_E}} - \sqrt{\frac{1}{1 + r_{PE}X_G}}\right] \tag{76}$$

Using Eq. (2), the values of $X$ in points A, B, E, and G can be expressed as functions of $r_{PA}$, $r_{PE}$, $E_I$, and $E_F$ ($E_I > E_F \geq 0$):

$$X_A = -\frac{E_I}{\mu + E_I r_{PA}}, \qquad X_B = -\frac{E_F}{\mu + E_F r_{PA}}$$
$$X_E = -\frac{E_I}{\mu + E_I r_{PE}}, \qquad X_G = -\frac{E_F}{\mu + E_F r_{PE}} \tag{77}$$

To prove that $\Delta v_{EG} > \Delta v_{AB}$, the function $(\Delta v_{EG} - \Delta v_{AB})/\sqrt{2\mu}$ is considered. The relationships (76) and (77) yield

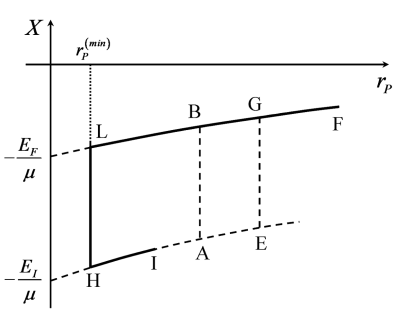


**Fig. 13 Globally optimal transfer between two hyperbolic trajectories.**

$$\frac{\Delta v_{EG}-\Delta v_{AB}}{\sqrt{2\mu}}=\frac{\sqrt{\mu+r_{PA}E_F}-\sqrt{\mu+r_{PA}E_I}}{\sqrt{r_{PA}}}+\frac{\sqrt{\mu+r_{PE}E_I}-\sqrt{\mu+r_{PE}E_F}}{\sqrt{r_{PE}}} \tag{78}$$

The auxiliary function $w(r_P)$ is now introduced as

$$w(r_P)=\frac{\sqrt{\mu+r_PE_I}-\sqrt{\mu+r_PE_F}}{\sqrt{r_P}} \tag{79}$$

and Eq. (78) can be rewritten as

$$\frac{\Delta v_{EG}-\Delta v_{AB}}{\sqrt{2\mu}}=w(r_{PE})-w(r_{PA}) \tag{80}$$

The derivative $\mathrm{d}w/\mathrm{d}r_P$ is given by

$$\frac{\mathrm{d}w}{\mathrm{d}r_P}=\frac{E_I-E_F}{\sqrt{\mu+r_PE_I}+\sqrt{\mu+r_PE_F}}\sqrt{\frac{\mu}{r_P(\mu+r_PE_I)(\mu+r_PE_F)}}$$
$$\Rightarrow \frac{\mathrm{d}w}{\mathrm{d}r_P}>0 \qquad \text{as } E_I>E_F \tag{81}$$

As $r_{PE}>r_{PA}$, Eqs. (10), (80), and (81) lead to the desired result:

$$\frac{\Delta v_{EG}-\Delta v_{AB}}{\sqrt{2\mu}}=w(r_{PE})-w(r_{PA})>0 \quad \Rightarrow \quad \Delta v_{EG}>\Delta v_{AB}$$
$$\forall\ (A,E) \quad \text{such that } r_{PE}>r_{PA}\geq 0 \tag{82}$$

Because points A and E are arbitrary, Eq. (82) proves that the minimum magnitude impulse corresponds to the minimum periapse radius (i.e., to the closest allowed approach to the attracting body). The preceding considerations lead to the identification of the globally optimal transfer from point I to point F, which is composed of the following three impulses:

1) One infinitesimal impulse at infinite distance while approaching the attracting body corresponds to arc IH.

2) One finite impulse at the minimum periapse radius corresponds to the vertical segment HL.

3) One infinitesimal impulse at infinite distance while leaving from the attracting body corresponds to arc LF.

Any other orbital transfer corresponds to a greater cost in terms of total velocity change. Moreover, due to the fact that the total cost of an optimal orbital transfer can be evaluated regardless of which is the initial and which is the final trajectory, the globally optimal transfer from point F to point I corresponds to path FLHI.

## V. Globally Optimal Transfers Between Elliptic Orbits and Escape Trajectories

This section addresses the determination of the globally optimal transfer between an elliptic orbit and an escape trajectory in the presence of constraints on the radius of closest approach to the attracting body and on the maximum apoapse radius of intermediate orbits:

$$r_P\geq r_P^{(\min)} \quad \text{and} \quad r_A\leq r_A^{(\max)} \Rightarrow X\geq X_{\min} \tag{83}$$

The latter inequality holds in the region of elliptic orbits only ($X>0$).

Because of these constraints in the $r_P$–$X$ plane, the shaded regions portrayed in Fig. 14 are not accessible; that is, no point representing an intermediate trajectory can be located inside these regions.

With reference to Fig. 14, to determine the globally optimal path from point I to point F, corresponding, respectively, to the initial elliptic orbit and to the final hyperbolic trajectory, the transfers IHF, IEADF, and IELGF are compared. However, due to the additive property (7) and to the fact that the points located on the same hyperbolic arc (i.e., points C, G, H, D, and F in Fig. 14) can be reached by means of infinitesimal impulses, paths EH, EAD, and ELG can be compared instead of transfers IHF, IEADF, and IELGF.

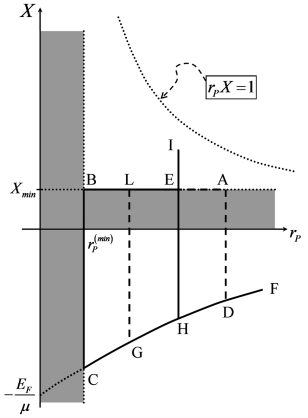


**Fig. 14 Globally optimal transfers from an elliptic orbit to an escape trajectory.**

As a first step, the inequality $\Delta v_{EAD}>\Delta v_{EH}$ will be demonstrated. To do this, the function $(\Delta v_{EAD}-\Delta v_{EH})/\sqrt{2\mu}$ is considered:

$$\frac{\Delta v_{EAD}-\Delta v_{EH}}{\sqrt{2\mu}}=\frac{(\Delta v_{EA}+\Delta v_{AD})-\Delta v_{EH}}{\sqrt{2\mu}}$$
$$=X_{\min}\left[\sqrt{\frac{r_{PA}}{1+r_{PA}X_{\min}}}-\sqrt{\frac{r_{PI}}{1+r_{PI}X_{\min}}}\right]+\frac{1}{\sqrt{r_{PA}}}\left[\frac{1}{\sqrt{1+r_{PA}X_D}}-\frac{1}{\sqrt{1+r_{PA}X_{\min}}}\right]-\frac{1}{\sqrt{r_{PI}}}\left[\frac{1}{\sqrt{1+r_{PI}X_H}}-\frac{1}{\sqrt{1+r_{PI}X_{\min}}}\right] \tag{84}$$

Using Eq. (2), the values of $X$ in points D and H can be expressed as functions of $r_{PA}>0$, $r_{PI}\geq 0$, and $E_F\geq 0$:

$$X_D=-\frac{E_F}{\mu+E_Fr_{PA}} \quad \text{and} \quad X_H=-\frac{E_F}{\mu+E_Fr_{PI}} \tag{85}$$

And Eq. (84) becomes

$$\frac{\Delta v_{EG}-\Delta v_{AB}}{\sqrt{2\mu}}=\left\{X_{\min}\sqrt{\frac{r_{PA}}{1+r_{PA}X_{\min}}}+\frac{1}{\sqrt{r_{PA}}}\left[\sqrt{\frac{\mu+r_{PA}E_F}{\mu}}-\frac{1}{\sqrt{1+r_{PA}X_{\min}}}\right]\right\}-\left\{X_{\min}\sqrt{\frac{r_{PI}}{1+r_{PI}X_{\min}}}+\frac{1}{\sqrt{r_{PI}}}\left[\sqrt{\frac{\mu+r_{PI}E_F}{\mu}}-\frac{1}{\sqrt{1+r_{PI}X_{\min}}}\right]\right\} \tag{86}$$

The auxiliary function $s(r_P)$ is now introduced as

$$s(r_P)\triangleq X_{\min}\sqrt{\frac{r_P}{1+r_PX_{\min}}}+\frac{1}{\sqrt{r_P}}\left[\sqrt{\frac{\mu+r_PE_F}{\mu}}-\frac{1}{\sqrt{1+r_PX_{\min}}}\right] \tag{87}$$

and Eq. (86) can be rewritten as

$$\frac{\Delta v_{EG}-\Delta v_{AB}}{\sqrt{2\mu}}=s(r_{PA})-s(r_{PI}) \tag{88}$$

To prove that $(\Delta v_{EAD}-\Delta v_{EH})>0$, the derivative $(\mathrm{d}s/\mathrm{d}r_P)$ is considered. The condition $(\mathrm{d}s/\mathrm{d}r_P)>0$ yields

$$(1+3r_PX_{\min})\sqrt{\mu+r_PE_F}>(1+r_PX_{\min})\sqrt{\mu(\mu+r_PX_{\min})} \tag{89}$$

After squaring and rearranging Eq. (89), one obtains

$$\frac{(3\xi+1)^2}{(\xi+1)^3} > \frac{\mu}{\mu + r_P E_F} \tag{90}$$

where $\xi \triangleq r_P X_{\min}$. The variable $\xi$ is constrained to the interval [0,1], due to the fact that $0 \le r_P X_{\min} \le 1$. The inequality (90) is satisfied for any value of $\xi$, because the function on the left-hand side of Eq. (90) is greater than 1 for all $\xi \in ]0, 1]$, whereas for the right-hand side, it follows that $0 < \mu/(\mu + r_P E_F) \le 1$.[‡] Therefore, the derivative $\mathrm{d}s/\mathrm{d}r_P$ is positive and this circumstance, through Eqs. (10) and (88), leads to the desired result:

$$\frac{\Delta v_{EAD} - \Delta v_{EH}}{\sqrt{2\mu}} = s(r_{PA}) - s(r_{PI}) > 0 \quad \Rightarrow \quad \Delta v_{EAD} > \Delta v_{EH}$$
$$\forall\ (A, E) \quad \text{such that } r_{PA} > r_{PE} = r_{PI} \ge 0 \tag{91}$$

Because point A is arbitrary, Eq. (91) proves that a transfer similar to transfer IEADF is not globally optimal. This means that starting from an ellipse with specified periapse radius $r_{PI}$, the globally optimal transfer to a hyperbolic trajectory does not include any intermediate elliptic orbit with a periapse radius greater than $r_{PI}$.

Path EH is compared with path ELG by defining the following function:

$$H(r_{PI}, r_{PL}) \triangleq \frac{\Delta v_{EH} - \Delta v_{ELG}}{\sqrt{2\mu}} = \frac{\Delta v_{EH} - (\Delta v_{EL} + \Delta v_{LG})}{\sqrt{2\mu}}$$
$$= \frac{1}{\sqrt{r_{PI}}}\left[\frac{1}{\sqrt{1 + r_{PI}X_H}} - \frac{1}{\sqrt{1 + r_{PI}X_{\min}}}\right] - X_{\min}\left[\sqrt{\frac{r_{PI}}{1 + r_{PI}X_{\min}}}\right.$$
$$\left. - \sqrt{\frac{r_{PL}}{1 + r_{PL}X_{\min}}}\right] - \frac{1}{\sqrt{r_{PL}}}\left[\frac{1}{\sqrt{1 + r_{PL}X_G}} - \frac{1}{\sqrt{1 + r_{PL}X_{\min}}}\right] \tag{92}$$

where the value of $X$ in point G is $-E_F/(\mu + E_F r_{PL})$. After introducing the expressions of $X_G$ and $X_H$ (written in terms of $r_{PI}$, $r_{PL}$, and $E_F$) into Eq. (92), one obtains

$$H(r_{PI}, r_{PL}) = \left\{\frac{1}{\sqrt{r_{PI}}}\left[\sqrt{\frac{\mu + r_{PI}E_F}{\mu}} - \frac{1}{\sqrt{1 + r_{PI}X_{\min}}}\right]\right.$$
$$\left. - X_{\min}\sqrt{\frac{r_{PI}}{1 + r_{PI}X_{\min}}}\right\} - \left\{\frac{1}{\sqrt{r_{PL}}}\left[\sqrt{\frac{\mu + r_{PL}E_F}{\mu}}\right.\right.$$
$$\left.\left. - \frac{1}{\sqrt{1 + r_{PL}X_{\min}}}\right] - X_{\min}\sqrt{\frac{r_{PL}}{1 + r_{PL}X_{\min}}}\right\} \tag{93}$$

The auxiliary function $m(r_P)$ is now defined as

$$m(r_P) \triangleq \frac{1}{\sqrt{r_P}}\left[\sqrt{\frac{\mu + r_P E_F}{\mu}} - \frac{1}{\sqrt{1 + r_P X_{\min}}}\right]$$
$$- X_{\min}\sqrt{\frac{r_P}{1 + r_P X_{\min}}} \tag{94}$$

and Eq. (78) can be simply rewritten as

$$H = m(r_{PI}) - m(r_{PL}) \tag{95}$$

To establish whether $(\Delta v_{EH} - \Delta v_{ELG}) > 0$ (i.e., $H > 0$), the derivative $\mathrm{d}m/\mathrm{d}r_P$ is considered:

$$\frac{\mathrm{d}m}{\mathrm{d}r_P} = \frac{1}{2r_P\sqrt{r_P}}\left[\frac{1}{\sqrt{1 + r_P X_{\min}}} - \sqrt{\frac{\mu}{\mu + r_P E_F}}\right] \tag{96}$$

The condition $(\mathrm{d}m/\mathrm{d}r_P) > 0$ yields

$$\frac{\mathrm{d}m}{\mathrm{d}r_P} > 0 \Rightarrow E_F > \mu X_{\min} \tag{97}$$

As a consequence, because point L is arbitrary, the transfer IEHF (equivalent to transfer IHF) is globally optimal if $E_F < \mu X_{\min}$. In fact, if the inequality $E_F < \mu X_{\min}$ holds, then from Eqs. (10), (95), and (97), it follows that $H < 0$, implying that $\Delta v_{IEH} < \Delta v_{IELG}\ \forall\ L$ such that $r_{PL} < r_{PI}$.

On the contrary, if $E_F > \mu X_{\min}$, then $\Delta v_{IEH} > \Delta v_{IELG}$ (i.e., $H > 0$), and the optimal value of $r_{PL}$ remains to be determined. This optimal value, denoted with $r^*_{PL}$, minimizes $\Delta v_{ELG}$. Such a requirement is equivalent to the maximization of $H$, which is defined by Eq. (92), because $\Delta v_{EH}$ is independent of $r_{PL}$ and $\Delta v_{ELG}$ is positive definite:

$$r^*_{PL} = \arg\min_{r_{PL}}\{\Delta v_{ELG}\} \Rightarrow r^*_{PL} = \arg\max_{r_{PL}}\{H\} \quad \text{if } H > 0$$
$$(\Leftrightarrow\ E_F > \mu X_{\min}) \tag{98}$$

To determine $r^*_{PL}$, the derivative of $H$ with respect to $r_{PL}$ is considered, under the assumption that $E_F > \mu X_{\min}$. From Eqs. (93), (96), and (97), it is evident that

$$\frac{\partial H}{\partial r_{PL}} \equiv -\left[\frac{\mathrm{d}m}{\mathrm{d}r_P}\right]_{r_P = r_{PL}} < 0 \tag{99}$$

Hence, the optimal value $r^*_{PL}$ coincides with the minimum allowed value for the periapse radius (i.e., $r^*_{PL} = r_P^{(\min)}$).

Thus, one concludes that, starting from an elliptic orbit, two possible globally optimal transfers to a hyperbolic trajectory exist, depending on the values of $X_{\min}$ and $E_F$:

1) If $E_F < \mu X_{\min}$, the transfer IHF is globally optimal. It is composed of one impulse at periapse (segment IH) and one infinitesimal impulse at infinite distance while leaving from the attracting body (arc HF).

2) If $E_F > \mu X_{\min}$, the transfer IEBCF is globally optimal. It is composed of: one impulse at periapse (segment IE), one impulse at the maximum apoapse radius (segment EB), one impulse at the minimum periapse radius (segment BC), and one infinitesimal impulse at infinite distance while leaving from the attracting body (arc CF).

This result is partially in contrast with that derived by Hazelrigg [18], who identified only path IEBCF as globally optimum. In addition, the optimal choice between the two options 1 and 2 turns out to be independent of $r_P^{(\min)}$. Of course, cases $X_{\min} = 0$ (no constraint on the radius of greatest recession), $r_P^{(\min)} = 0$ (no constraint on the radius of closest approach), and $X_F = 0$ (transfer from an elliptic orbit to a parabolic trajectory) can be deduced as special cases.

As a final remark, due to the interchangeability of points I and F (with regard to the total cost of the transfer), the globally optimal paths from point F to point I are transfer FHI (if $E_F < \mu X_{\min}$) and transfer FCBEI (if $E_F > \mu X_{\min}$).

## VI. Conclusions

This work offers a complete analysis of angle-free, time-free orbital transfers by covering all of the possible cases of impulsive transfers between two coplanar Keplerian trajectories. The investigation described in this paper leads to the determination of the number and magnitudes of the impulsive changes of velocity that perform the global optimal transfer in each specific case. The major results of this research are summarized in the following.

With regard to ellipse-to-ellipse transfers, the Hohmann transfer and the bielliptic transfer with maximum apoapse radius of the midcourse trajectory are both globally optimal. This property is proved through a direct approach, which is based only on ordinary calculus in conjunction with a simple graphical procedure. The final selection between these two transfers depends on the apoapse and periapse radii of the terminal orbits. This issue is addressed through a direct analytical procedure that is capable of taking into account all

[‡]The degenerate case $E_F = 0$ and $X_{\min} = 0$ corresponds to the transfer to a parabolic trajectory; in this context, paths EH and AD are equivalent.

ellipse-to-ellipse transfers, with the possible constraint on the radius of greatest recession. However, in general, the Hohmann transfer turns out to be unequivocally globally optimal if $1/9 < r_{PF}/r_{PI} < 9$ (where $r_{PF}$ and $r_{PI}$ denote the periapse radii of the final and the initial orbits, respectively), whereas it is outperformed by an arbitrary bielliptic transfer if $r_{PF}/r_{PI} > 15.582$ or $r_{PF}/r_{PI} < 0.06418$. This paper demonstrates that analytical expressions exist for all of the limiting values of $r_{PF}/r_{PI}$ that unequivocally determine the global optimality of either the Hohmann transfer or the bielliptic transfer. With reference to terminal circular orbits, the Hohmann transfer is more economical than the biparabolic transfer if $0.08376 < r_{PF}/r_{PI} < 11.939$. This latter result is well known in the scientific literature and can be easily verified through the method described in this research.

Globally optimal transfers involving escape trajectories have also been investigated. The related results have been obtained again through the use of ordinary calculus in conjunction with simple graphical constructions. The globally optimal transfer between two hyperbolic trajectories is performed through a single (finite) impulse, which occurs at the minimum periapse radius (i.e., at the radius of allowed closest approach to the attracting body). The global optimal transfer from an elliptic orbit to an escape trajectory is performed either through a two-impulse sequence or through a four-impulse transfer. In this case, the final choice between the two options depends only on the radius of greatest recession (of intermediate orbits) and on the energy of the hyperbolic trajectory, whereas it turns out to be independent of the minimum allowed periapse radius.

The fundamental features of all globally optimal transfers are derived in a way that is general, simpler, and more direct than existing studies in the literature, because only ordinary calculus and graphical procedures are employed to demonstrate the results of interest.

## Appendix A: Impulsive Changes of Velocity on Hyperbolic Trajectories

In general, the application of an in-plane impulsive change of velocity on a hyperbolic trajectory modifies its semimajor axis (SMA) $a$, its eccentricity $e$, and its orientation with respect to an inertial frame. It will be demonstrated in this Appendix that an infinitesimal impulse at infinite distance is capable of changing the eccentricity $e$ (i.e., the magnitude of the specific angular momentum $h$ and the periapse radius $r_P$) without modifying the SMA $a$ (and therefore the trajectory energy $E$). To do this, one can consider the orbital frame $(\hat{r}, \hat{\theta}, \hat{h})$, defined by the unit vectors $\hat{r}$, which is aligned with the position vector, and $\hat{h}$, which is aligned with the specific angular momentum $\mathbf{h}(=\mathbf{r}\times\mathbf{v})$. In this frame, the position vector $\mathbf{r}$ and the velocity vector $\mathbf{v}$ can be written as follows:

$$\mathbf{r} = r\hat{r} = \frac{a(1-e^2)}{1+e\cos f}\hat{r} \tag{A1}$$

$$\mathbf{v} = v_r\hat{r} + v_\theta\hat{\theta} = \left[\sqrt{\frac{\mu}{a(1-e^2)}}e\sin f\right]\hat{r} + \left[\sqrt{\frac{\mu}{a(1-e^2)}}(1+e\cos f)\right]\hat{\theta} \tag{A2}$$

The true anomaly $f$ for hyperbolic trajectories varies in the following range:

$$-\arccos\left(-\frac{1}{e}\right) < f < \arccos\left(-\frac{1}{e}\right) \tag{A3}$$

Let the subscripts $-$ and $+$ denote the values of a variable immediately before and after the application of an impulsive change of velocity $\mathbf{\Delta v}$, which is assumed to be directed along $\hat{\theta}$ (i.e., $\mathbf{\Delta v} = \Delta v_\theta\hat{\theta}$). The position vector is continuous across the impulse:

$$\mathbf{r}_- = r_-\hat{r} = \frac{a_-(1-e_-^2)}{1+e_-\cos f_-}\hat{r} = \mathbf{r}_+ = r_+\hat{r} = \frac{a_+(1-e_+^2)}{1+e_+\cos f_+}\hat{r} \tag{A4}$$

And the velocity vector $\mathbf{v}$ is modified:

$$\begin{aligned}\mathbf{v}_+ &= \left[\sqrt{\frac{\mu}{a_+(1-e_+^2)}}e_+\sin f_+\right]\hat{r} + \left[\sqrt{\frac{\mu}{a_+(1-e_+^2)}}(1+e_+\cos f_+)\right]\hat{\theta} = \mathbf{v}_- + \Delta v_\theta\hat{\theta}\\ &= \left[\sqrt{\frac{\mu}{a_-(1-e_-^2)}}e_-\sin f_-\right]\hat{r} + \left[\sqrt{\frac{\mu}{a_-(1-e_-^2)}}(1+e_-\cos f_-) + \Delta v_\theta\right]\hat{\theta}\end{aligned} \tag{A5}$$

Equations (A4) and (A5) yield three scalar relationships:

$$e_+\cos f_+ = \frac{a_+(1-e_+^2)}{a_-(1-e_-^2)}(1+e_-\cos f_-) - 1 \tag{A6}$$

$$e_+\sin f_+ = \sqrt{\frac{a_+(1-e_+^2)}{a_-(1-e_-^2)}}e_-\sin f_- \tag{A7}$$

$$\Delta v_\theta = \sqrt{\frac{\mu}{a_-(1-e_-^2)}}(1+e_-\cos f_-)\left[\sqrt{\frac{a_+(1-e_+^2)}{a_-(1-e_-^2)}} - 1\right] \tag{A8}$$

If the eccentricities $e_-$ and $e_+$, the SMA of the initial hyperbolic trajectory $a_-$, and the true anomaly $f_-$, which identifies the point at which the impulse is applied, are assumed to be specified, analytical expressions for $a_+$, $\Delta v_\theta$, and $f_+$ (in terms of $e_-$, $e_+$, $a_-$, and $f_-$) can be derived.

After squaring and adding Equations (A6) and (A7), one obtains

$$a_+^2(e_+^2-1)(1+e_-\cos f_-)^2 + a_+a_-(e_-^2-1)[e_-^2 - 1 - (1+e_-\cos f_-)^2] - a_-^2(e_-^2-1)^2 = 0 \tag{A9}$$

This equation has the following (negative) root:

$$a_+ = \frac{-a_-(e_-^2-1)}{2(e_+^2-1)(1+e_-\cos f_-)^2}\{g(e_-,f_-) - \sqrt{g^2(e_-,f_-) + 4(e_+^2-1)(1+e_-\cos f_-)^2}\} \tag{A10}$$

where $g(e_-,f_-) = e_-^2 - 1 - (1+e_-\cos f_-)^2$. After some rearrangement, Eq. (A10) becomes

$$\begin{aligned}a_+ &= \frac{-a_-(e_-^2-1)}{2(e_+^2-1)(1+e_-\cos f_-)^2}\cdot\frac{g^2(e_-,f_-) - [g^2(e_-,f_-) + 4(e_+^2-1)(1+e_-\cos f_-)^2]}{g(e_-,f_-) + \sqrt{g^2(e_-,f_-) + 4(e_+^2-1)(1+e_-\cos f_-)^2}}\\ &= \frac{2a_-(e_-^2-1)}{e_-^2 - 1 - (1+e_-\cos f_-)^2 + \sqrt{[e_-^2 - 1 - (1+e_-\cos f_-)^2]^2 + 4(e_+^2-1)(1+e_-\cos f_-)^2}}\end{aligned} \tag{A11}$$

Finally, $f_+$ and $\Delta v_\theta$ can be calculated through Eqs. (A7) and (A8). Figure A1 shows an example of the effect of a finite impulse $\Delta v_\theta \hat{\theta}$, applied at finite distance while approaching the attracting body: the SMA $a$ and the eccentricity $e$ are modified, as well as the orientation of the conic, which is rotated by an angle $\phi$. As $\mathbf{r}_- \equiv \mathbf{r}_+$, angle $\phi$ is given simply by

$$\phi = f_- - f_+ \tag{A12}$$

where $\phi < 0$ in Fig. A1.

The application of an impulse at infinite distance (while approaching the attracting body) corresponds to $f_- \to -\arccos(-1/e_-)$. In the limit as $f_- \to -\arccos(-1/e_-)$, from Eq. (A11), one obtains

$$\lim_{f_- \to -\arccos(-1/e_-)} a_+ = a_- \tag{A13}$$

That is, the SMA $a_+$ resulting from the application of $\Delta v_\theta \hat{\theta}$ coincides with $a_-$, regardless of $e_-$ and $e_+$. This also means that the trajectory energy $E$ remains unaltered. In this limiting situation, the asymptotes of the hyperbolic trajectories [for $f_- \to -\arccos(-1/e_-)$ and $f_+ \to -\arccos(-1/e_+)$] are parallel, as shown in Fig. A2. The angle of rotation $\phi$ is given by

$$\phi = \arccos\left[-\frac{1}{e_-}\right] - \arccos\left[-\frac{1}{e_+}\right] \tag{A14}$$

where $\phi < 0$ in Fig. A2.

Finally, the impulse magnitude $\Delta v_\theta$ can be evaluated through Eq. (A8):

$$\lim_{f_- \to -\arccos(-1/e_-)} \Delta v_\theta = \lim_{f_- \to -\arccos(-1/e_-)} \left\{ \sqrt{\frac{\mu}{a_-(1-e_-^2)}} \times (1 + e_- \cos f_-)\left[ \sqrt{\frac{a_+(1-e_+^2)}{a_-(1-e_-^2)}} - 1 \right] \right\} = 0 \tag{A15}$$

where $a_+ \to a_-$ as $f_- \to -\arccos(-1/e_-)$. From Eqs. (A13) and (A15), one concludes that an infinitesimal impulse at infinite distance is capable of arbitrarily changing the eccentricity (from $e_-$ to $e_+$) without modifying the SMA $a$, and therefore the trajectory energy $E = -\mu/2a$. This circumstance is related to the direction of the impulse, which becomes perpendicular to $\mathbf{v}$ as $r \to \infty$. With reference to the representation of Fig. 1, this fact implies that in the $r_P$–$X$ plane, orbital transfers along hyperbolic arcs of constant energy $[E = -\mu X/(1 + X r_P)]$ can be performed (ideally) without any cost.

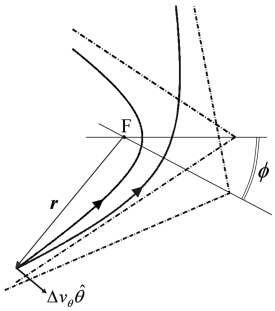


**Fig. A1 Application of an impulsive change of velocity at finite distance on a hyperbolic trajectory.**

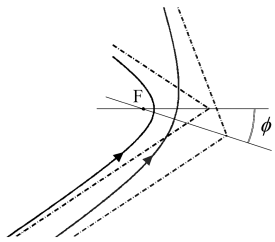


**Fig. A2 Application of an infinitesimal impulse at infinite distance on a hyperbolic trajectory.**

Of course, the application of an infinitesimal impulse at infinite distance is concretely infeasible and represents the limiting case of a finite feasible impulse as the distance from the attracting body tends to infinity. However, the preceding result proves that arbitrary changes of the periapse radius of a hyperbolic trajectory can be performed through the application of arbitrarily modest impulses at relevant distances, without producing any substantial variation of the trajectory energy.

As a final remark, all of the results derived for $f_- \to -\arccos(-1/e_-)$ can be obtained in the same way for the symmetric situation corresponding to $f_- \to \arccos(-1/e_-)$.

## Appendix B: Limiting Values of $\beta$

This Appendix is concerned with the formal derivation of the limiting values of $\beta$ (i.e., $\beta_S^{(\min)}$, $\beta_D$, $\beta_E$, $\beta_N^{(\max)}$, $\beta_B$, and $\beta_A$), which define the regions of global optimality of Hohmann and bielliptic transfers, as discussed in Sec. III. These extremal values of $\beta$ are located over specific curves $Z(\alpha_{\min}, \alpha_B, \beta) = 0$. In particular, four curves must be considered:

1) The curve corresponding to $Z(\alpha_{\min} = 0, \alpha_B, \beta)|_{\beta>1} = 0$ determines $\beta_A$ and $\beta_E$.

2) The curve corresponding to $Z(\alpha_{\min} = 0, \alpha_B, \beta)|_{\beta<1} = 0$ determines $\beta_B$ and $\beta_D$.

3) The curve corresponding to $Z(\alpha_{\min} = 1/\beta_N^{(\max)}, \alpha_B, \beta)|_{\beta>1} = 0$ determines $\beta_N^{(\max)}$.

4) The curve corresponding to $Z(\alpha_{\min} = 1, \alpha_B, \beta)|_{\beta<1} = 0$ determines $\beta_S^{(\min)}$.

### I. $Z(\alpha_{\min} = 0, \alpha_B, \beta)|_{\beta>1} = 0$

Using Eq. (49) with $\alpha_{\min} = 0$ and $\beta > 1$, the equation $Z = 0$ assumes the following form:

$$\frac{\alpha_B - 1}{\sqrt{1+\alpha_B}} + 1 + \frac{1}{\sqrt{\beta}} - \sqrt{\frac{1+\alpha_B\beta}{\beta}} = 0 \quad \Rightarrow \quad \frac{\alpha_B - 1}{\sqrt{1+\alpha_B}} + 1 = \sqrt{\frac{1+\alpha_B\beta}{\beta}} - \frac{1}{\sqrt{\beta}} \tag{B1}$$

The value $\beta_A$ corresponds to the point at which the curve $Z = 0$ intersects the hyperbola $\alpha_B\beta = 1$. After replacing $\alpha_B$ with $1/\beta$, Eq. (B1) becomes

$$\frac{1-\beta}{\sqrt{\beta(\beta+1)}} + 1 + \frac{1}{\sqrt{\beta}} - \sqrt{\frac{2}{\beta}} = 0 \tag{B2}$$

As $\beta > 1$, Eq. (B2) is equivalent to

$$\sqrt{\beta(\beta+1)} + (1-\sqrt{2})\sqrt{\beta+1} = \beta - 1 \tag{B3}$$

After squaring and rearranging Eq. (B3) 2 times, one obtains the following third-degree equation:

$$(3-2\sqrt{2})\beta^3 - (5-2\sqrt{2})\beta^2 - (7-6\sqrt{2})\beta - 3 + 2\sqrt{2} = 0 \tag{B4}$$

which coincides with Eq. (69) after dividing by $(3-2\sqrt{2})$. The value $\beta_A (\approx 11.939)$ represents one of the roots of Eq. (69) (the only root in the range of $\beta > 1$).

It will now be demonstrated that an explicit form exists for the function $\hat{\beta}(\alpha_B)$, defined implicitly by

$$Z(\alpha_{\min} = 0, \alpha_B, \hat{\beta})|_{\hat{\beta}>1} = 0$$

To do this, the relationship (B1) is considered again. After squaring Eq. (B1) 2 times, one obtains $\beta$ as a function of $\alpha_B$:

$$\beta = \hat{\beta}(\alpha_B) = \frac{(\alpha_B+1)[\alpha_B^2-\alpha_B+2+2(\alpha_B-1)\sqrt{\alpha_B+1}]}{(\alpha_B-1)^2(\alpha_B+2-2\sqrt{\alpha_B+1})} \quad \text{(B5)}$$

This expression is singular in the limit as $\alpha_B \to 0$. However, one can recognize that

$$\begin{aligned}\hat{\beta}(\alpha_B) &= \frac{(\alpha_B+1)[1-\alpha_B-\sqrt{\alpha_B+1}]^2}{(\alpha_B-1)^2(\sqrt{\alpha_B+1}-1)^2} \\ &= \frac{(\alpha_B+1)(\sqrt{\alpha_B+1}+1)^2[(1-\alpha_B)^2-(\alpha_B+1)]^2}{(\alpha_B-1)^2(1-\alpha_B+\sqrt{\alpha_B+1})^2[(\alpha_B+1)-1]^2}\end{aligned} \quad \text{(B6)}$$

Finally, Eq. (B6) simplifies to yield the more compact expression:

$$\hat{\beta}(\alpha_B) = \frac{(\alpha_B+1)(3-\alpha_B)^2}{(\alpha_B-1)^2}\left[\frac{\sqrt{1+\alpha_B}+1}{\sqrt{1+\alpha_B}+1-\alpha_B}\right]^2 \quad \text{(B7)}$$

This expression is not singular as $\alpha_B \to 0$, because from Eq. (B7), it follows that $\hat{\beta}(0) = 9$, thus proving also that the limiting value $\beta_E$ is exactly equal to 9.

**II. $Z(\alpha_{\min}=0, \alpha_B, \beta)|_{\beta<1} = 0$**

Using Eq. (49) with $\alpha_{\min} = 0$ and $\beta < 1$, the equation $Z = 0$ assumes the following form:

$$\begin{aligned}&\sqrt{1+\alpha_B}-1+\frac{1-\alpha_B\beta}{\sqrt{\beta(1+\alpha_B\beta)}}-\frac{1}{\sqrt{\beta}}=0 \quad \Rightarrow \\ &\sqrt{1+\alpha_B}-1=\frac{1}{\sqrt{\beta}}-\frac{1-\alpha_B\beta}{\sqrt{\beta(1+\alpha_B\beta)}}\end{aligned} \quad \text{(B8)}$$

After squaring Eq. (B8) 2 times, the following third-degree equation can be deduced:

$$F_3(\alpha)\beta^3 + F_2(\alpha)\beta^2 + F_1(\alpha)\beta + F_0(\alpha) = 0 \quad \text{(B9)}$$

where

$$F_0(\alpha) = -(\sqrt{1+\alpha_B}-1)^2 \quad \text{(B10)}$$

$$F_1(\alpha) = 2\alpha_B^2 + \alpha_B + 2 - 2\sqrt{1+\alpha_B} \quad \text{(B11)}$$

$$F_2(\alpha) = \alpha_B[4\alpha_B - \alpha_B^2 + 4 - 2(2+\alpha_B)\sqrt{1+\alpha_B}] \quad \text{(B12)}$$

$$F_3(\alpha) = \alpha_B^2(\sqrt{1+\alpha_B}-1)^2 \quad \text{(B13)}$$

One of the three roots of Eq. (B9) corresponds to the curve portrayed in Fig. 10b (corresponding to $\alpha_{\min} = 0$). The value $\beta_B$ corresponds to the point at which this curve intersects the straight line $\alpha_B = 1$. Therefore, $\beta_B$ represents one of the roots of Eq. (B9) when $\alpha_B$ is set to 1:

$$(3-2\sqrt{2})\beta^3 + (7-6\sqrt{2})\beta^2 + (5-2\sqrt{2})\beta - 3 + 2\sqrt{2} = 0 \quad \text{(B14)}$$

which coincides with Eq. (71) after dividing by $(3-2\sqrt{2})$. From Eq. (71), one obtains $\beta_B \approx 0.08376$ (and this is the only root in the range of $0 < \beta < 1$). The same steps do not allow determining $\beta_D$, because Eq. (B9) is trivially satisfied for $\alpha_B = 0$. However, Eq. (B8) can be rewritten as

$$\begin{aligned}&[(1+\alpha_B)-1]\Big/\left[\frac{1}{\beta}-\frac{(1-\alpha_B\beta)^2}{\beta(1+\alpha_B\beta)}\right] \\ &\quad = (\sqrt{1+\alpha_B}+1)\Big/\left[\frac{1}{\sqrt{\beta}}+\frac{1-\alpha_B\beta}{\sqrt{\beta(1+\alpha_B\beta)}}\right]\end{aligned} \quad \text{(B15)}$$

The left-hand side of Eq. (B15) simplifies to

$$\frac{1+\alpha_B\beta}{3-\alpha_B\beta} = (\sqrt{1+\alpha_B}+1)\Big/\left(\frac{1}{\sqrt{\beta}}+\frac{1-\alpha_B\beta}{\sqrt{\beta(1+\alpha_B\beta)}}\right) \quad \text{(B16)}$$

Letting $\alpha_B = 0$, one obtains

$$\tfrac{1}{3} = \sqrt{\beta} \Rightarrow \beta = \tfrac{1}{9} \quad \text{(B17)}$$

Hence, the limiting value $\beta_D$ is equal to 1/9: $\beta_D = 1/9 \approx 0.1111$, as formerly stated in Sec. III.

**III. $Z(\alpha_{\min}=1/\beta_N^{(\max)}, \alpha_B, \beta)|_{\beta>1} = 0$**

With reference to Fig. 9, $\beta_N^{(\max)}$ is the limiting value of $\beta$ in point N over the hyperbola $\alpha_B\beta = 1$ as $\alpha_{\min} \to 1/\beta$. What will be demonstrated is that $\beta_N^{(\max)}$ is one of the roots of Eq. (74). To do this, the expression of $Z = 0$ for $\alpha_B = 1/\beta$ is first deduced:

$$\begin{aligned}&\sqrt{\frac{2}{\beta}}-\sqrt{\frac{1+\alpha_{\min}\beta}{\beta}}-\frac{1-\beta}{\sqrt{\beta(\beta+1)}}+\frac{\alpha_{\min}-1}{\sqrt{\alpha_{\min}+1}}=0 \\ &\Rightarrow \sqrt{\frac{2}{\beta}}-\sqrt{\frac{1+\alpha_{\min}\beta}{\beta}}=\frac{1-\beta}{\sqrt{\beta(\beta+1)}}-\frac{\alpha_{\min}-1}{\sqrt{\alpha_{\min}+1}}\end{aligned} \quad \text{(B18)}$$

If $\alpha_{\min} = 1/\beta$ is substituted in Eq. (B18), then Eq. (B18) is trivially satisfied and this circumstance prevents deriving $\beta_N^{(\max)}$. To overcome this difficulty, Eq. (B18) can be rewritten as follows:

$$\begin{aligned}&\left(\frac{2}{\beta}-\frac{1+\alpha_{\min}\beta}{\beta}\right)\Big/\left(\frac{(1-\beta)^2}{\beta(\beta+1)}-\frac{(\alpha_{\min}-1)^2}{\alpha_{\min}+1}\right) \\ &\quad = \left(\sqrt{\frac{2}{\beta}}+\sqrt{\frac{1+\alpha_{\min}\beta}{\beta}}\right)\Big/\left(\frac{1-\beta}{\sqrt{\beta(\beta+1)}}+\frac{\alpha_{\min}-1}{\sqrt{\alpha_{\min}+1}}\right)\end{aligned} \quad \text{(B19)}$$

The left-hand side of Eq. (B19) now simplifies to

$$\begin{aligned}&\frac{(\alpha_{\min}+1)(\beta+1)}{\alpha_{\min}+\alpha_{\min}\beta+1-3\beta} \\ &\quad = \left(\sqrt{\frac{2}{\beta}}+\sqrt{\frac{1+\alpha_{\min}\beta}{\beta}}\right)\Big/\left(\frac{1-\beta}{\sqrt{\beta(\beta+1)}}+\frac{\alpha_{\min}-1}{\sqrt{\alpha_{\min}+1}}\right)\end{aligned} \quad \text{(B20)}$$

Letting $\alpha_{\min} = 1/\beta$, Eq. (B20) becomes

$$\frac{(\beta+1)^2}{1+2\beta-3\beta^2} = \frac{\sqrt{2(\beta+1)}}{1-\beta} \quad \text{(B21)}$$

After squaring Eq. (B21), one obtains the following third-degree equation:

$$\beta^3 - 15\beta^2 - 9\beta - 1 = 0 \quad \text{(B22)}$$

which coincides with Eq. (74). The value $\beta_N^{(\max)}(\approx 15.582)$ represents one of the roots of Eq. (B22) (the only root in the range of $\beta > 1$).

**IV. $Z(\alpha_{\min}=1, \alpha_B, \beta)|_{\beta<1} = 0$**

With reference to Fig. 9, $\beta_S^{(\min)}$ is the limiting value of $\beta$ in $S$ over the segment LM as $\alpha_{\min} \to 1$. It will be demonstrated that $\beta_S^{(\min)}$ is one of the roots of Eq. (75). To do this, the expression of $Z = 0$ for $\alpha_B = 1$ is deduced:

$$\frac{1-\alpha_{\min}\beta}{\sqrt{\beta(1+\alpha_{\min}\beta)}}-\frac{1-\beta}{\sqrt{\beta(\beta+1)}}-\sqrt{2}+\sqrt{\alpha_{\min}+1}=0$$

$$\Rightarrow \frac{1-\alpha_{\min}\beta}{\sqrt{\beta(1+\alpha_{\min}\beta)}}-\frac{1-\beta}{\sqrt{\beta(\beta+1)}}=\sqrt{2}-\sqrt{\alpha_{\min}+1} \quad \text{(B23)}$$

Also in this case, if $\alpha_{\min}=1$ is substituted in Eq. (B23), then Eq. (B23) is trivially satisfied and this circumstance prevents deriving $\beta_S^{(\min)}$. To overcome this difficulty, Eq. (B23) can be rewritten as follows:

$$\left(\frac{(1-\alpha_{\min}\beta)^2}{\beta(1+\alpha_{\min}\beta)}-\frac{(1-\beta)^2}{\beta(\beta+1)}\right)\Bigg/[2-(\alpha_{\min}+1)]$$
$$=\left(\frac{1-\alpha_{\min}\beta}{\sqrt{\beta(1+\alpha_{\min}\beta)}}+\frac{1-\beta}{\sqrt{\beta(\beta+1)}}\right)\Bigg/(\sqrt{2}+\sqrt{\alpha_{\min}+1}) \quad \text{(B24)}$$

The left-hand side of Eq. (B24) now simplifies to

$$\frac{3-\beta(\alpha_{\min}+1)-\alpha_{\min}\beta^2}{(\beta+1)(1+\alpha_{\min}\beta)}$$
$$=\left(\frac{1-\alpha_{\min}\beta}{\sqrt{\beta(1+\alpha_{\min}\beta)}}+\frac{1-\beta}{\sqrt{\beta(\beta+1)}}\right)\Bigg/(\sqrt{2}+\sqrt{\alpha_{\min}+1}) \quad \text{(B25)}$$

Letting $\alpha_{\min}=1$, Eq. (B25) becomes

$$\frac{\beta+3}{(\beta+1)^2}=\frac{1}{\sqrt{2\beta(\beta+1)}} \quad \text{(B26)}$$

After squaring Eq. (B26), one obtains the following third-degree equation:

$$\beta^3+9\beta^2+15\beta-1=0 \quad \text{(B27)}$$

which coincides with Eq. (75). The value $\beta_S^{(\min)}(\approx 0.06418)$ represents one of the roots of Eq. (B27) (the only root in the range of $0<\beta<1$).

## References


[1] Robbins, H. M., "Analytical Study of the Impulsive Approximation," *AIAA Journal*, Vol. 4, No. 8, 1966, pp. 1417–1423. doi:10.2514/3.3687

[2] Zee, C., "Effects of Finite Thrusting Time in Orbit Maneuvers," *AIAA Journal*, Vol. 1, No. 1, 1963, pp. 60–64. doi:10.2514/3.1469

[3] Hohmann, W., *Die Erreichbarkeit der Himmelskoerper*, Oldenbourg, Munich, 1925; also "The Attainability of Heavenly Bodies," NASA translation TT-F-44, 1960.

[4] Hoelker, R. F., and Silber, R., "The Bi-Elliptical Transfer Between Coplanar Circular Orbits," *Proceedings of the 4th Symposium on Ballistic Missiles and Space Technology*, Vol. 3, Pergamon, New York, 1961, pp. 164–175.

[5] Shternfeld, A., *Soviet Space Science*, Basic Books, New York, 1959, pp. 109–111.

[6] Edelbaum, T. N., "Some Extensions of the Hohmann Transfer Maneuver," *ARS Journal*, Vol. 29, 1959, pp. 864–865.

[7] Ting, L., "Optimum Orbital Transfer by Impulses," *ARS Journal*, Vol. 30, 1960, pp. 1013–1018.

[8] Ting, L., "Optimum Orbital Transfer by Several Impulses," *Astronautica Acta*, Vol. 6, No. 5, 1960, pp. 256–265.

[9] Lawden, D. F., "Optimal Powered Arcs in an Inverse Square Law Field," *ARS Journal*, Vol. 31, 1961, pp. 566–568.

[10] Lawden, D. F., *Optimal Trajectories for Space Navigation*, Butterworths, London, 1963, pp. 79–110.

[11] Barrar, R. B., "An Analytic Proof that the Hohmann-Type Transfer is the True Minimum Two-Impulse Transfer," *Astronautica Acta*, Vol. 9, No. 1, 1963, pp. 1–11.

[12] Moyer, H. G., "Minimum Impulse Coplanar Circle-Ellipse Transfer," *AIAA Journal*, Vol. 3, No. 4, 1965, pp. 723–726. doi:10.2514/3.2954

[13] Marec, J.-P., *Optimal Space Trajectories*, Elsevier, Amsterdam, 1979, pp. 21–27.

[14] Battin, R. H., *An Introduction to the Mathematics and Methods of Astrodynamics*, AIAA Education Series, AIAA, New York, 1987, pp. 529–530.

[15] Palmore, J. I., "An Elementary Proof the Optimality of Hohmann Transfers," *Journal of Guidance, Control, and Dynamics*, Vol. 7, No. 5, 1984, pp. 629–630. doi:10.2514/3.56375

[16] Prussing, J. E., "Simple Proof the Global Optimality of the Hohmann Transfer," *Journal of Guidance, Control, and Dynamics*, Vol. 15, No. 4, 1992, pp. 1037–1038. doi:10.2514/3.20941

[17] Yuan, F., and Matsushima, K., "Strong Hohmann Transfer Theorem," *Journal of Guidance, Control, and Dynamics*, Vol. 18, No. 2, 1995, pp. 371–373. doi:10.2514/3.21394

[18] Hazelrigg, G. A., "Globally Optimal Impulsive Transfers via Green's Theorem," *Journal of Guidance, Control, and Dynamics*, Vol. 7, No. 4, 1984, pp. 462–470. doi:10.2514/3.19879

[19] Lawden, D. F., "Optimal Intermediate-Thrust Arcs in a Gravitational Field," *Astronautica Acta*, Vol. 8, 1962, pp. 106–123.

[20] Kopp, R. E., and Moyer, H. G., "Necessary Conditions for Singular Extremals," *AIAA Journal*, Vol. 3, No. 8, 1965, pp. 1439–1444. doi:10.2514/3.3165

[21] Robbins, H. M., "Optimality of Intermediate Thrust Arcs of Rocket Trajectories," *AIAA Journal*, Vol. 3, No. 6, 1965, pp. 1094–1098. doi:10.2514/3.3060

[22] Bell, D. J., and Jacobson, D. H., *Singular Optimal Control Problems*, Academic Press, London, 1975, pp. 72–81.

[23] Gurley, J. G., "Optimal-Thrust Trajectories in an Arbitrary Gravitational Field," *SIAM Journal on Control*, Vol. 2, No. 3, 1964, pp. 423–432. doi:10.1137/0302033

[24] Goh, B. S., "The Second Variation for the Singular Bolza Problem," *SIAM Journal on Control*, Vol. 4, No. 2, 1966, pp. 309–325. doi:10.1137/0304026

[25] Winn, C. B., "Minimum Fuel Transfers Between Coaxial Orbits, Both Coplanar and Noncoplanar," American Astronautical Society Paper 66-119, 1966.

[26] Prussing, J. E., and Conway, B. A., *Orbital Mechanics*, Oxford Univ. Press, New York, 1993, pp. 108–112.

[27] Marchal, C., "Transferts Optimaux Entre Orbites Elliptiques Coplanaires (Durée Indifférente)," *Astronautica Acta*, Vol. 11, No. 6, 1965, pp. 432–445.